

DARK MATTER

ASTR 333/433

TODAY

CLUSTERS OF GALAXIES

Homework 3 due

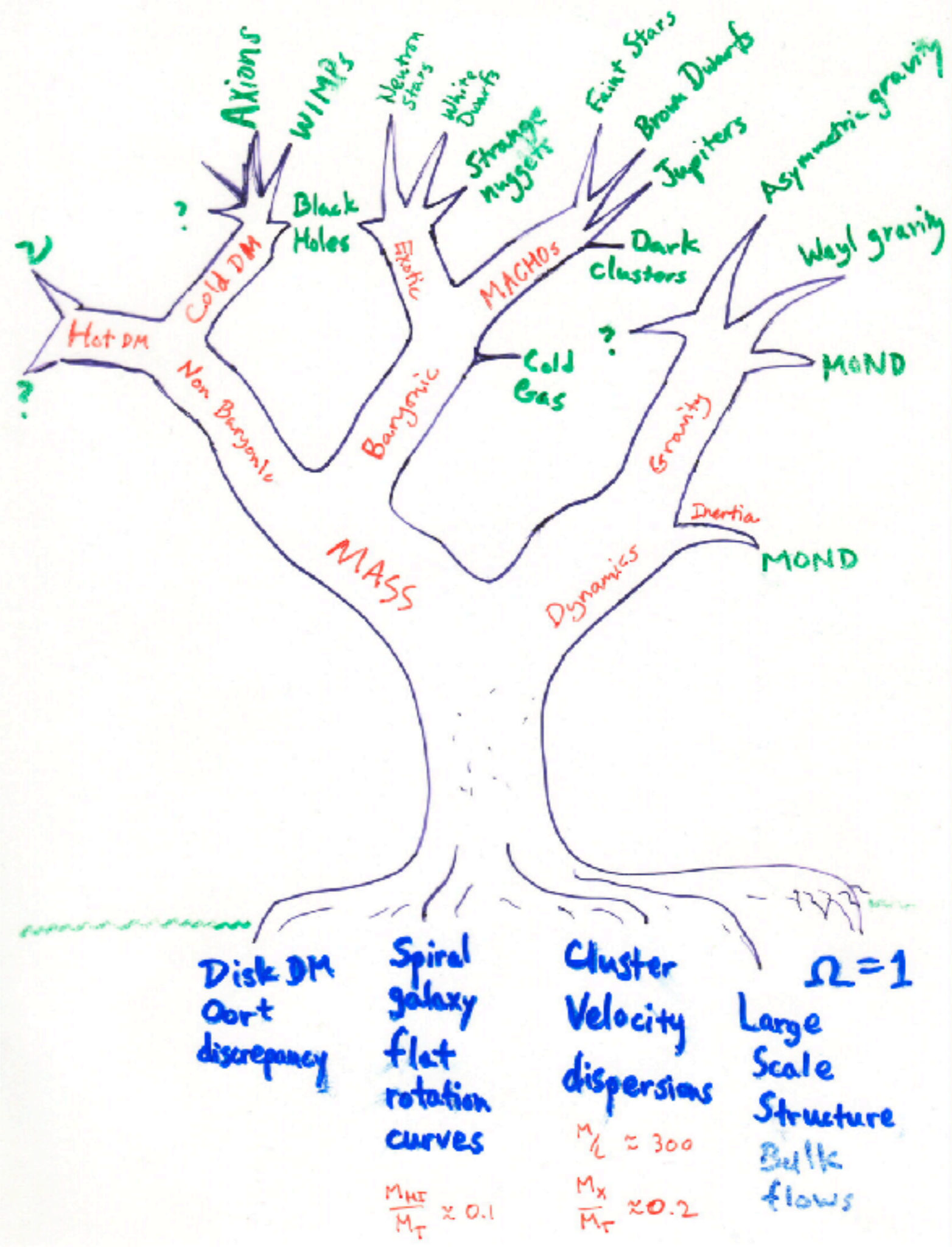
ASTR 433 Projects

4/17: distribute abstracts

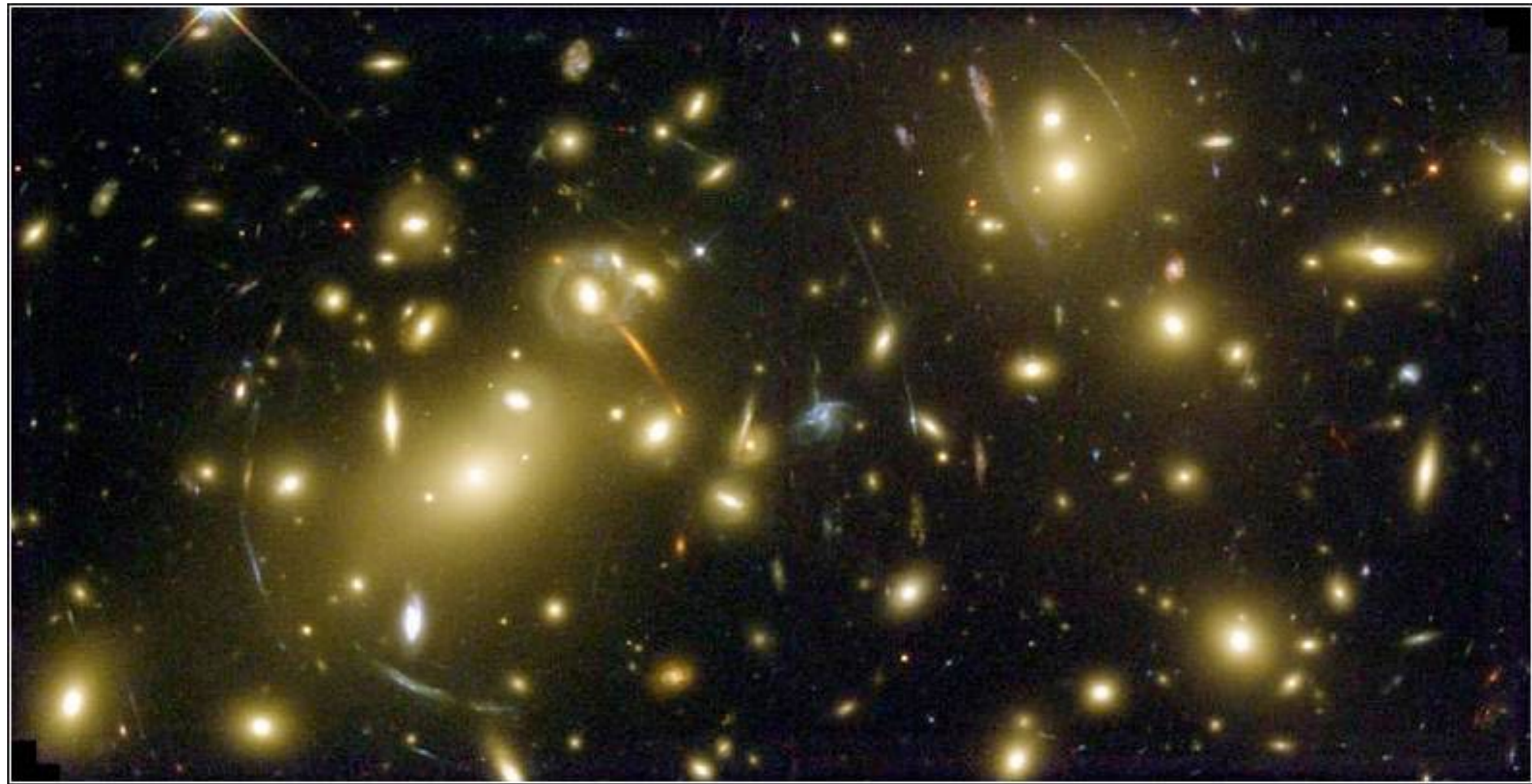
4/19: 20 minute talks

4/24: Homework 4 due

4/26: Exam

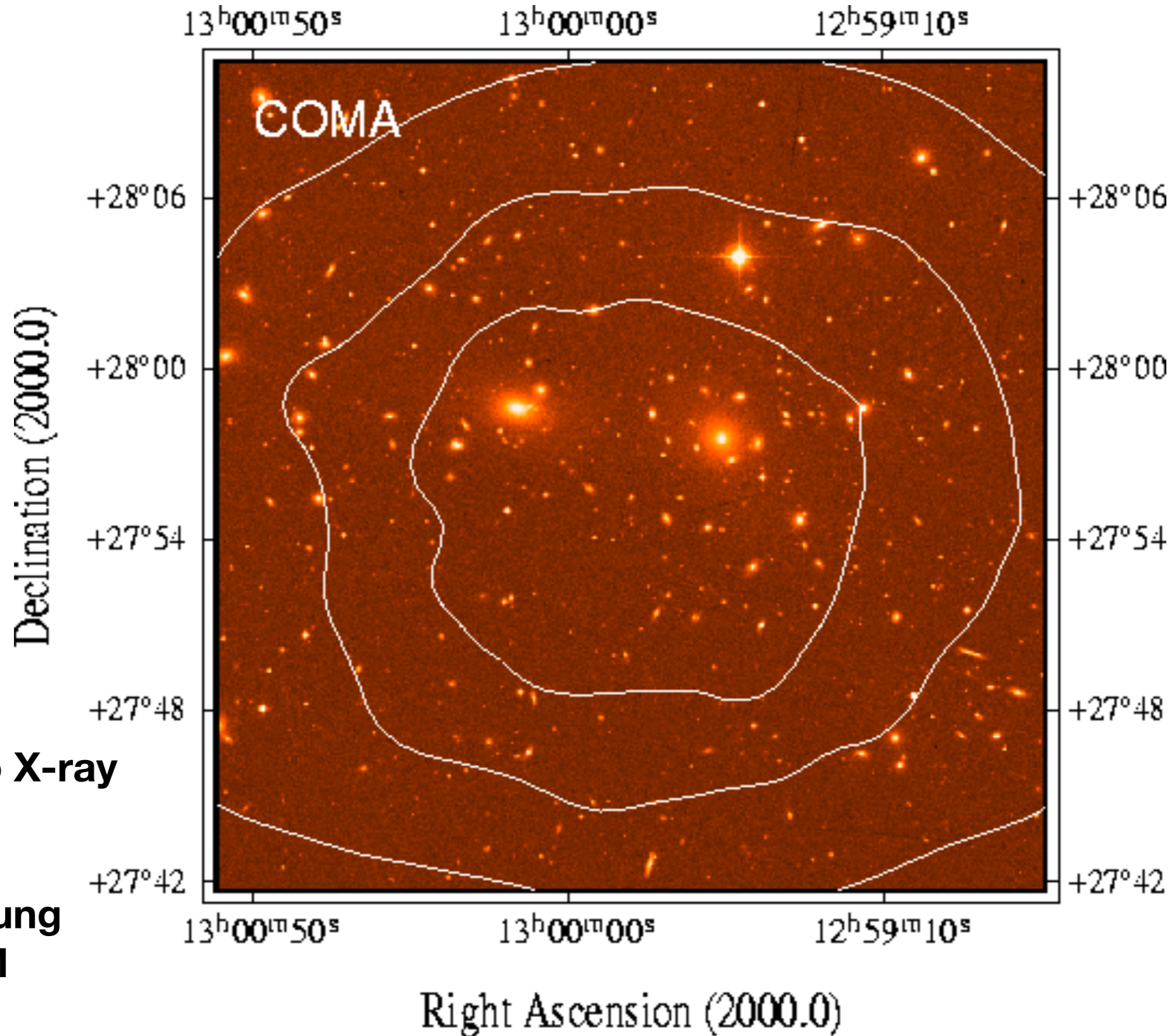


Galaxy Clusters



4 distinct measures: velocity dispersion, gravitational lensing, hydrostatic equilibrium of X-ray gas, and the Sunyaev-Zel'dovich effect

Clusters in optical and X-ray (contours)



Typically two X-ray sources

Bremsstrahlung from hot ICM

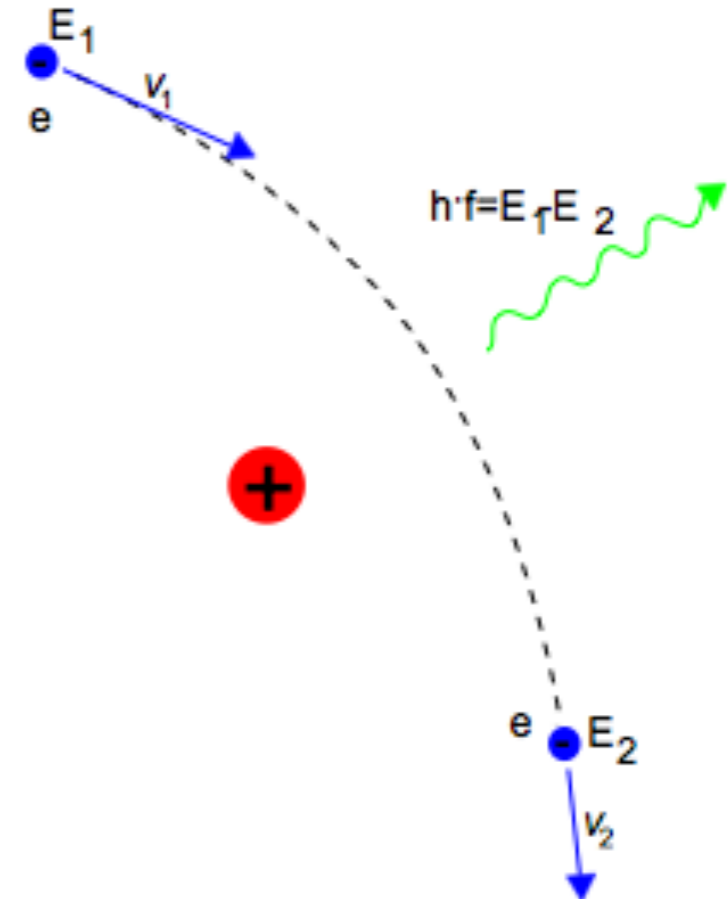
AGN and other point sources

Bremsstrahlung

Gas falling into clusters shock heats to the virial temperature of the potential, $kT \sim mV^2$ resulting in an intracluster medium (ICM) composed of hot plasma. This plasma radiates in X-rays via Bremsstrahlung (braking radiation).

[Sometimes also called free-free radiation]

Just classical radiation from accelerated charges.



Global correlations in galaxy clusters

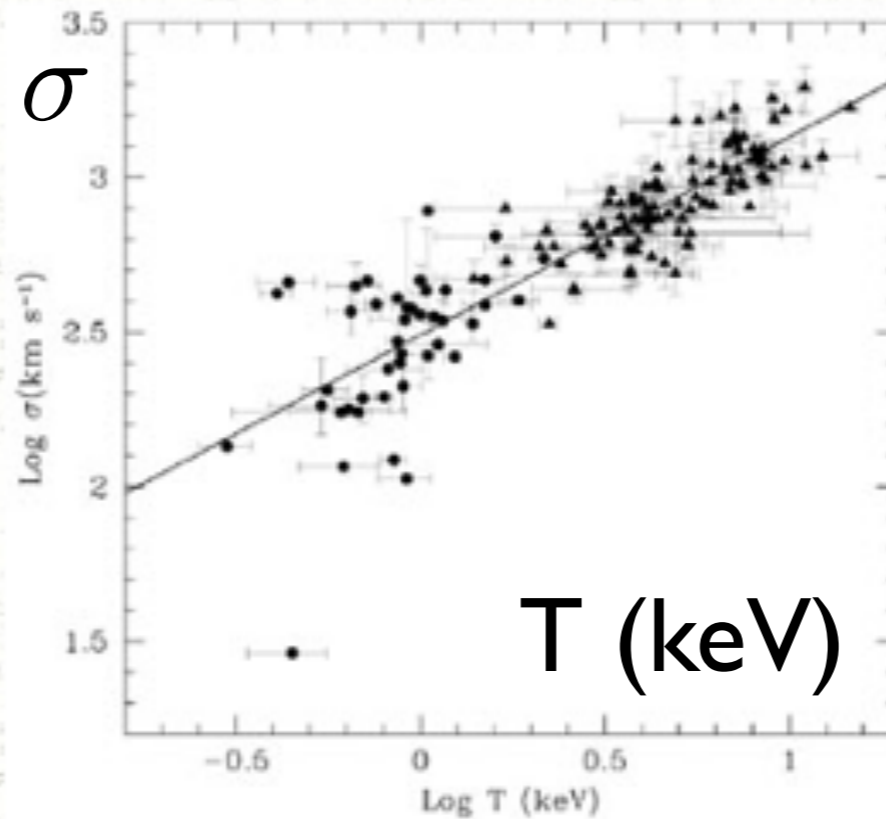


Figure 4. Logarithm of the X-ray temperature versus logarithm of optical velocity dispersion for a sample of groups (circles) and clusters (triangles). The group data are taken from the literature compilation of [Xue & Wu \(2000\)](#), with the addition of the groups in [Helsdon & Ponman \(2000\)](#). The cluster data are taken from [Wu et al \(1999\)](#). The solid line represents the best-fit found by [Wu et al \(1999\)](#) for the clusters sample (using an orthogonal distance regression method). Within the large scatter, the groups are consistent with the cluster relationship.

Global correlations in galaxy clusters

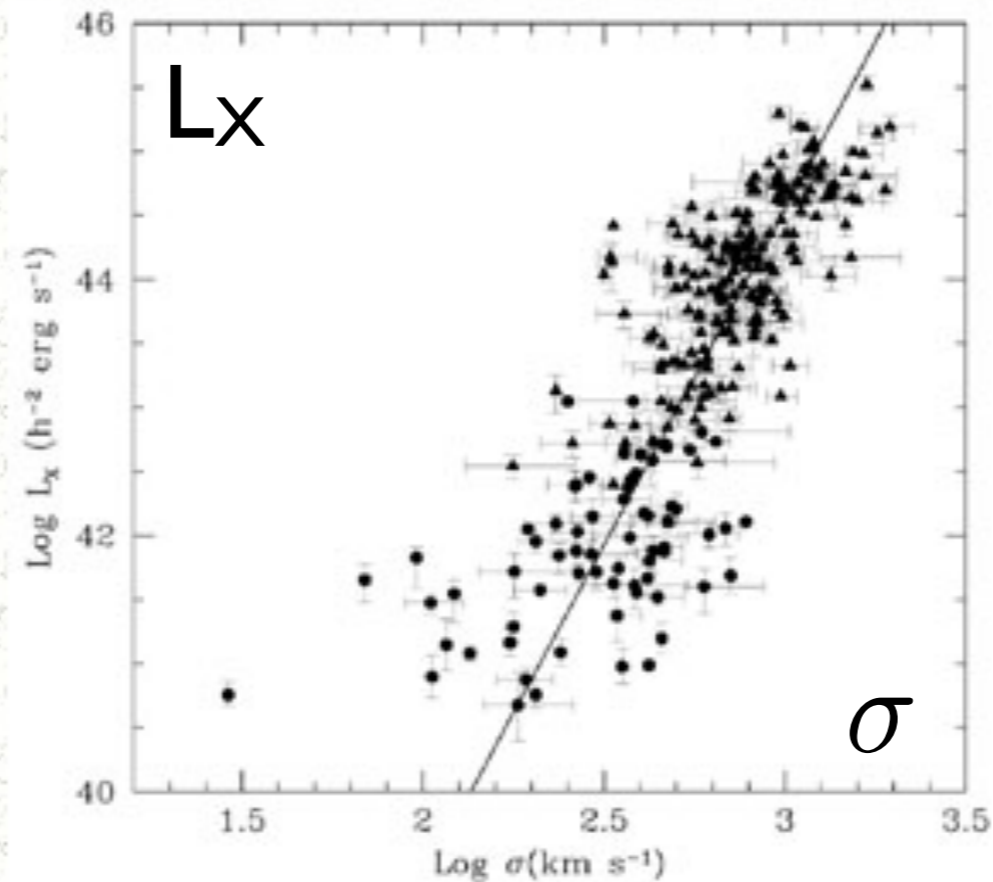


Figure 5. Logarithm of optical velocity dispersion versus logarithm of X-ray luminosity for a sample of groups (circles) and clusters (triangles). The data are taken from the same sources cited in [Figure 4](#). The solid line represents the best-fit found by [Wu et al \(1999\)](#) for the clusters sample (using an orthogonal distance regression method).

Global correlations in galaxy clusters

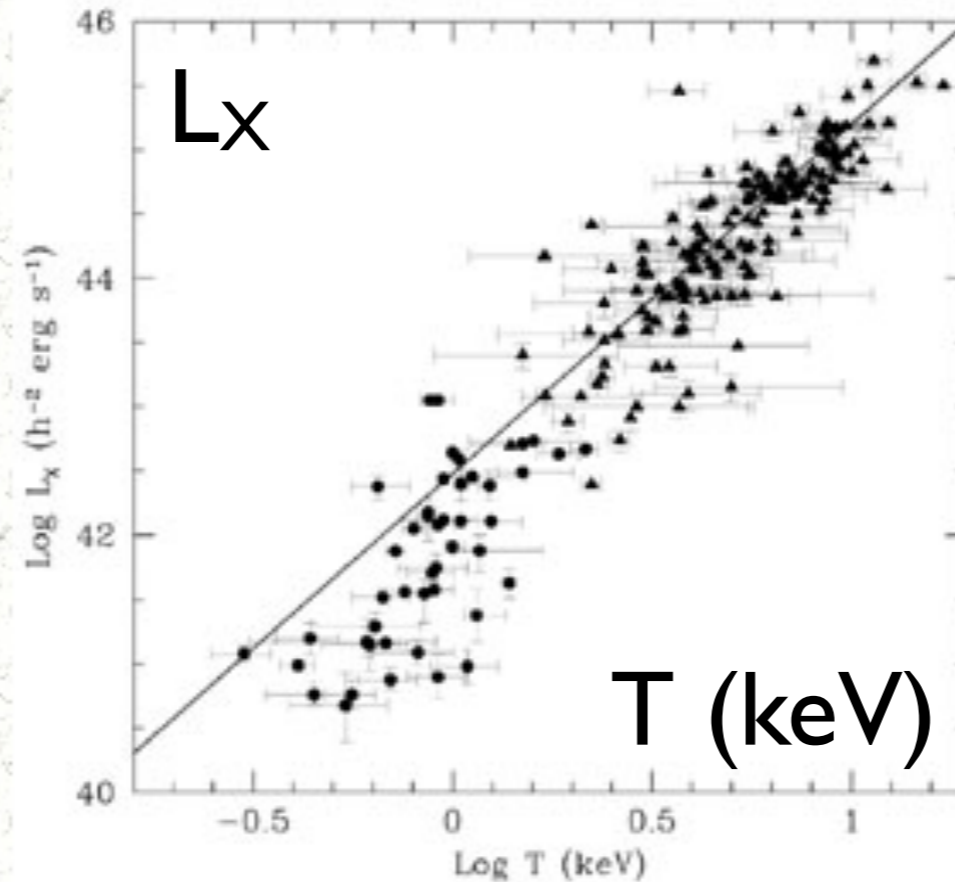


Figure 6. Logarithm of the X-ray temperature versus logarithm of X-ray luminosity for a sample of groups (circles) and clusters (triangles). The data are taken from the same sources cited in [Figure 4](#). The solid line represents the best-fit found by [Wu et al \(1999\)](#) for the clusters sample (using an orthogonal distance regression method). The observed relationship for groups is somewhat steeper than the best-fit cluster relationship.

Beta models

The X-ray surface brightness at a projected radius R
for an isothermal sphere is given by:

$$S(R) = S_0 \left[1 + (R/r_c)^2 \right]^{-3\beta + 1/2}$$

S_0 central surface brightness

r_c core radius of gas distribution

$$\beta \equiv \frac{\mu m_p \sigma^2}{k T_g} = \frac{\text{specific energy in galaxies}}{\text{specific energy in the hot gas}}$$

$$\beta \equiv \frac{\mu m_p \sigma^2}{k T_g} = \frac{\text{specific energy in galaxies}}{\text{specific energy in the hot gas}}$$

μ is the mean molecular weight

m_p is the mass of the proton

σ is the one-dimensional velocity dispersion of the galaxies

T_g is the temperature of the ICM

Typically the gas is assumed to be isothermal

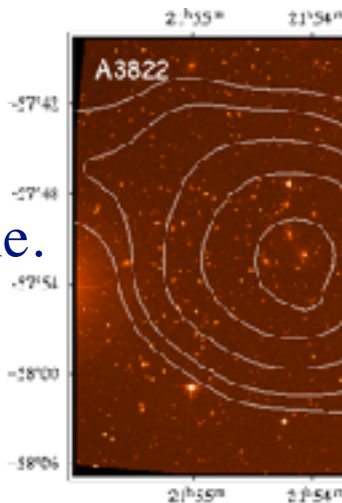
β treated as fit parameter; typically $\sim 2/3$
BUT often higher when sigma well measured
and often lower in groups

Mass Estimator

$$M_{tot}(< R) = \frac{kT_g(R)}{G\mu m_p} \left[\frac{\partial \log \rho}{\partial \log r} + \frac{\partial \log T}{\partial \log r} \right] R$$

the gas density profile is determined by fitting the standard beta model to the surface brightness profile.

the gas temperature is measured directly from the X-ray spectrum



Assumes

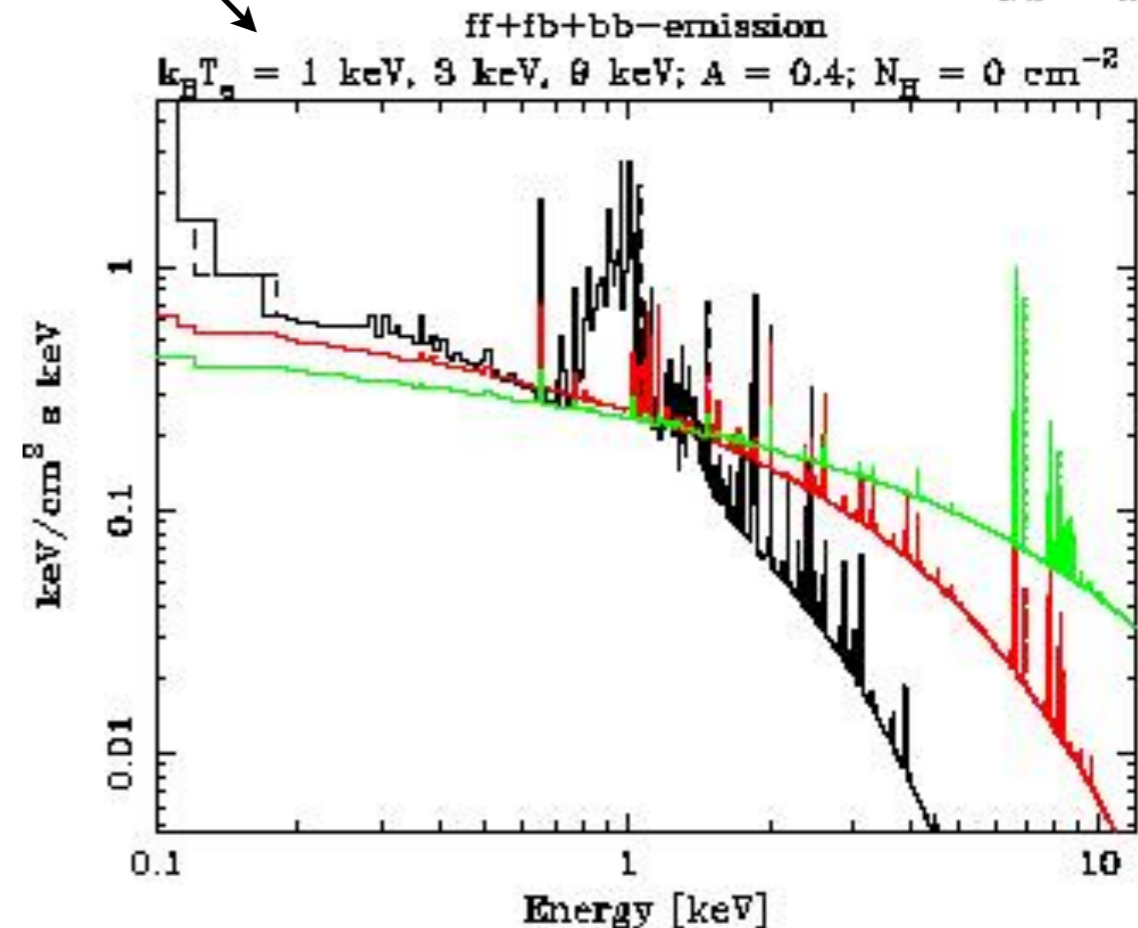
hydrostatic equilibrium

sphericity

often assumes

isothermality

$$\longrightarrow \frac{\partial \log T}{\partial \log r} = 0$$

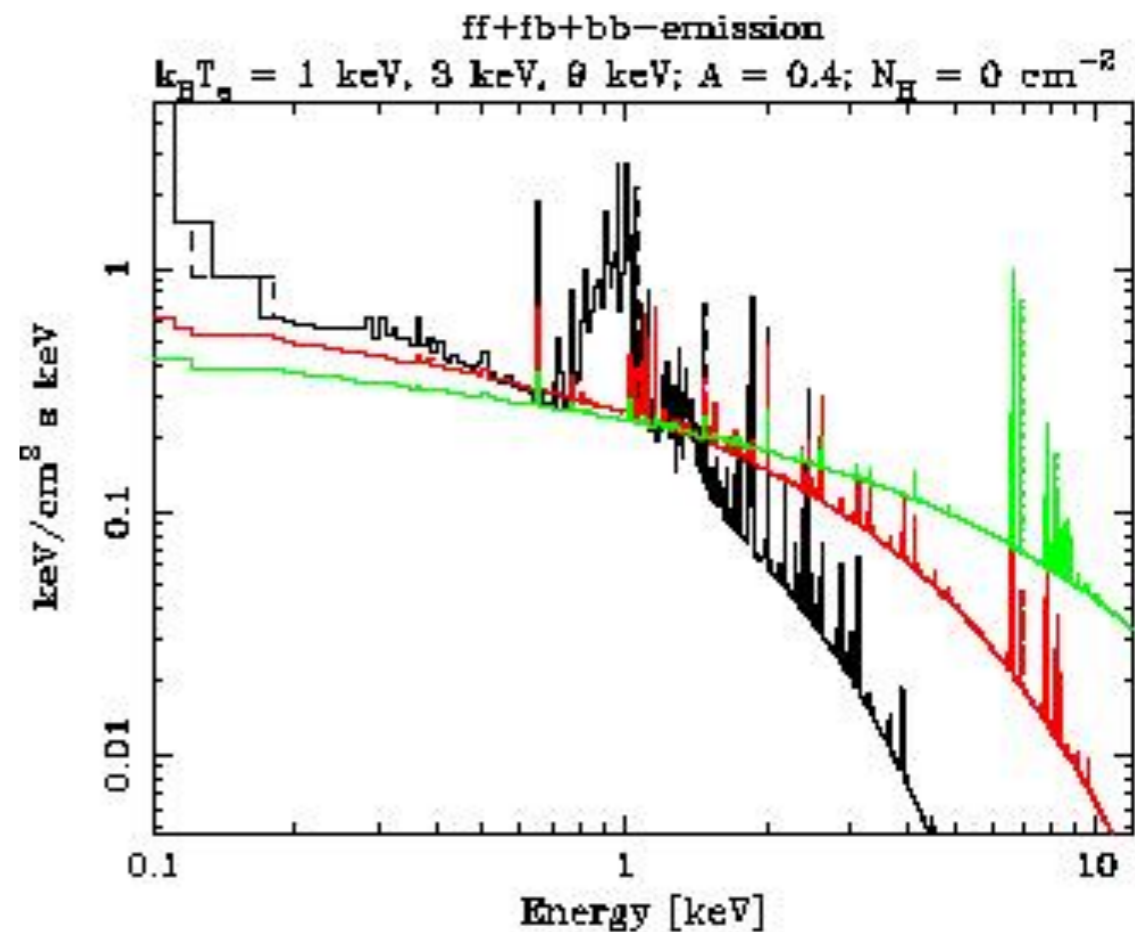


Mass Estimator

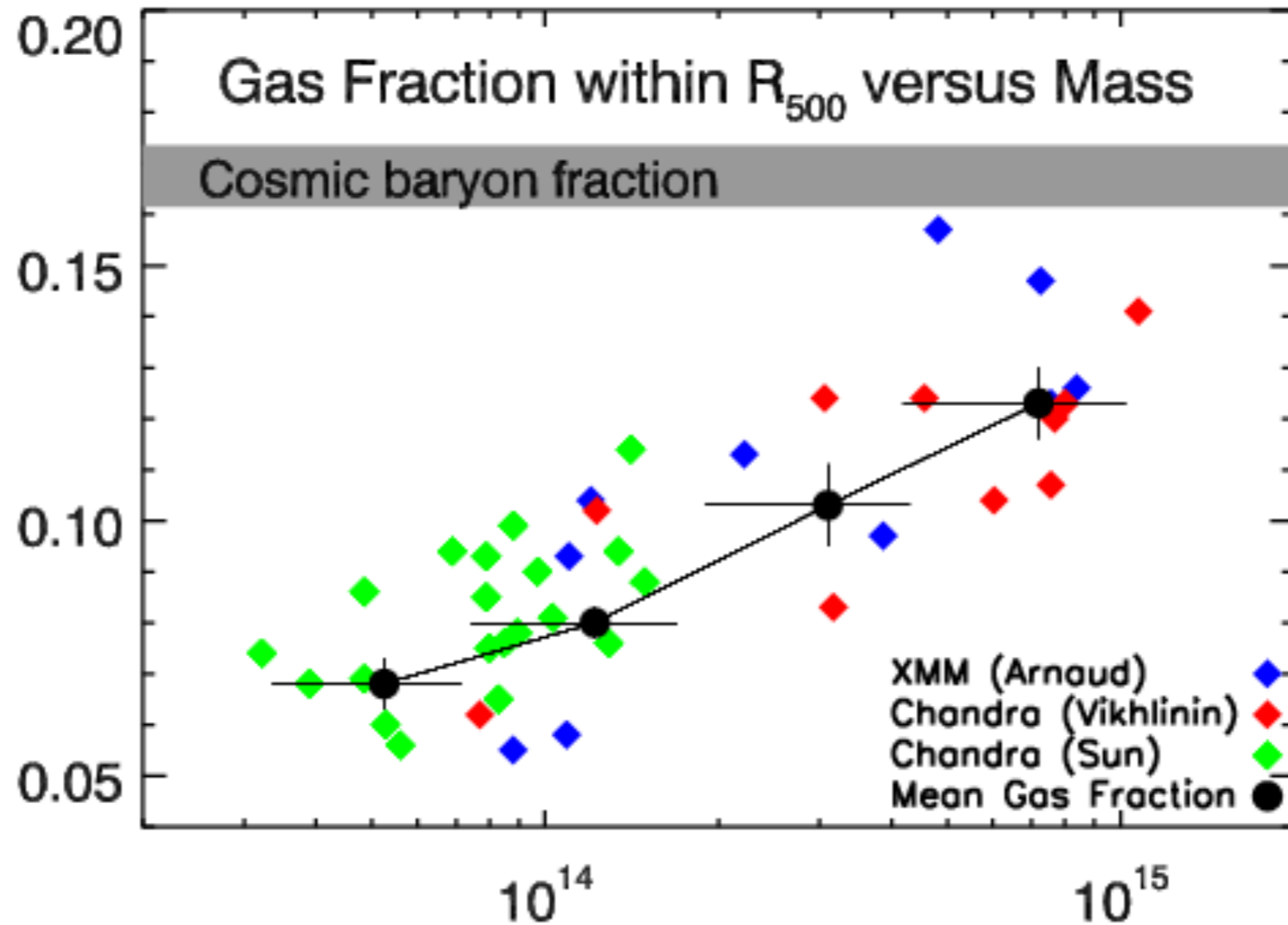
$$M_{tot}(< R) = \frac{kT_g(R)}{G\mu m_p} \left[\frac{\partial \log \rho}{\partial \log r} + \frac{\partial \log T}{\partial \log r} \right] R$$

basically,

$$M_{tot}(< R) \sim T_{gas} R$$



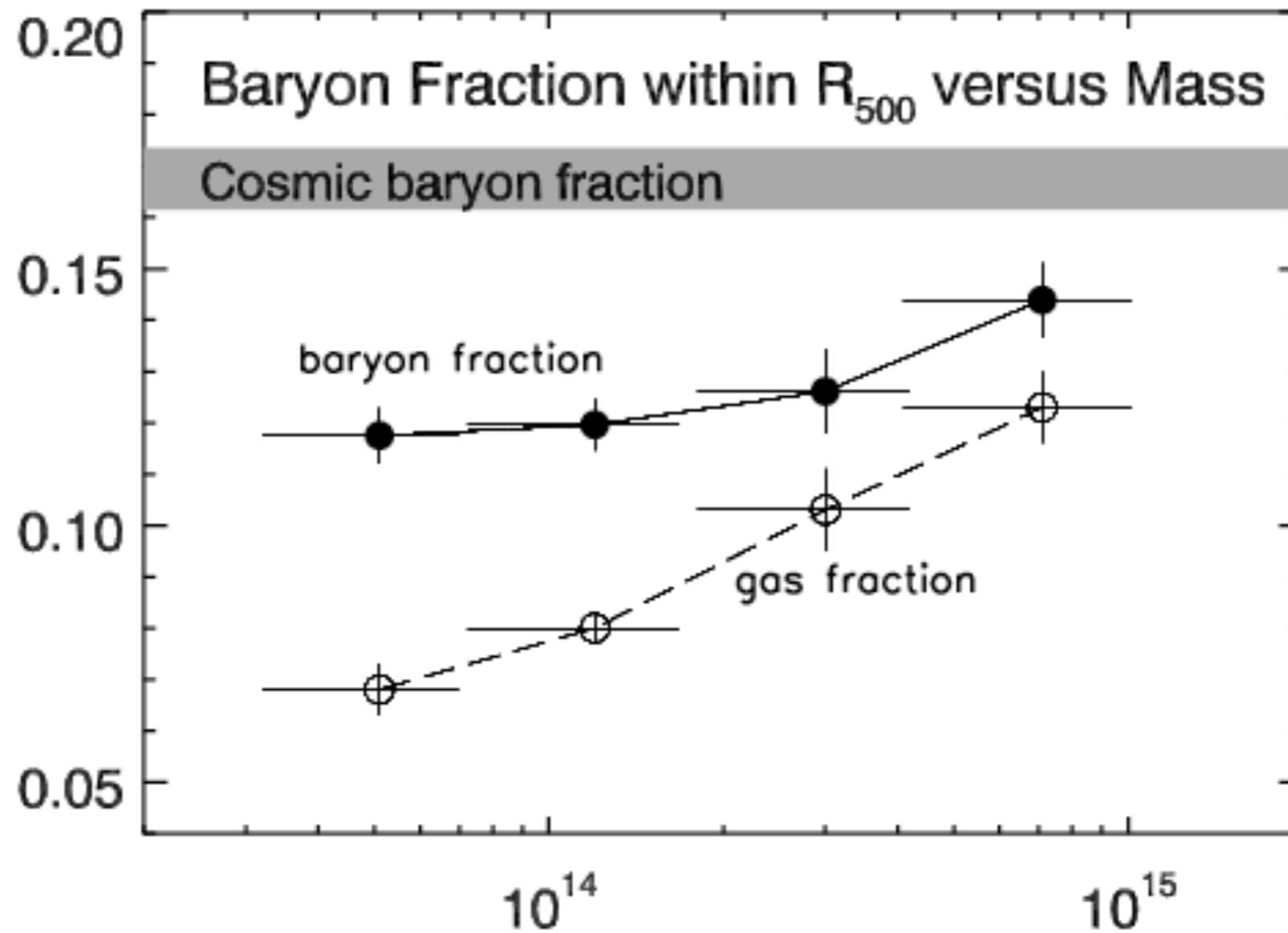
Rasheed (2010)



Typical result:

clusters have close to, but not quite, the expected baryon fraction

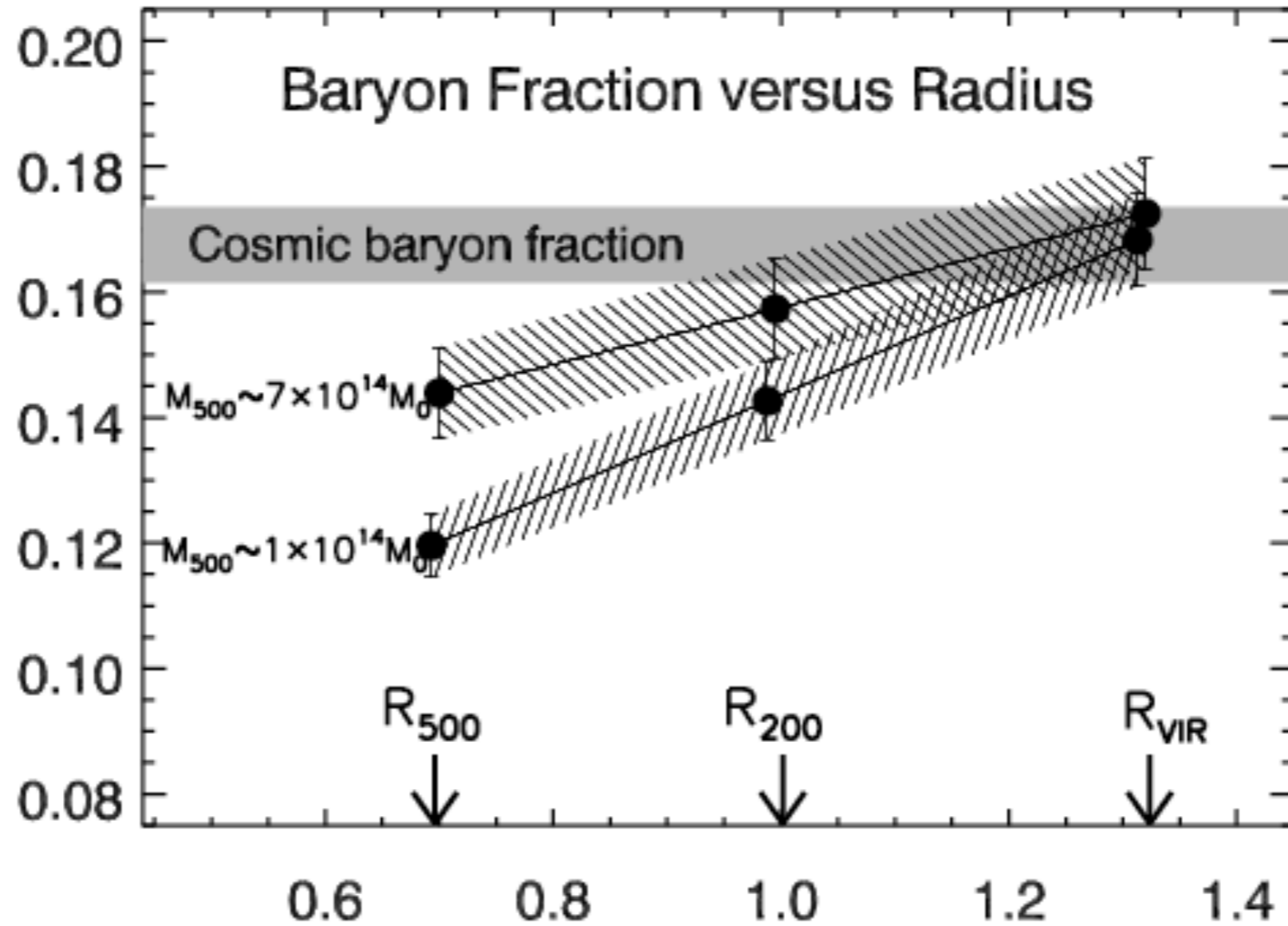
Rasheed (2010)



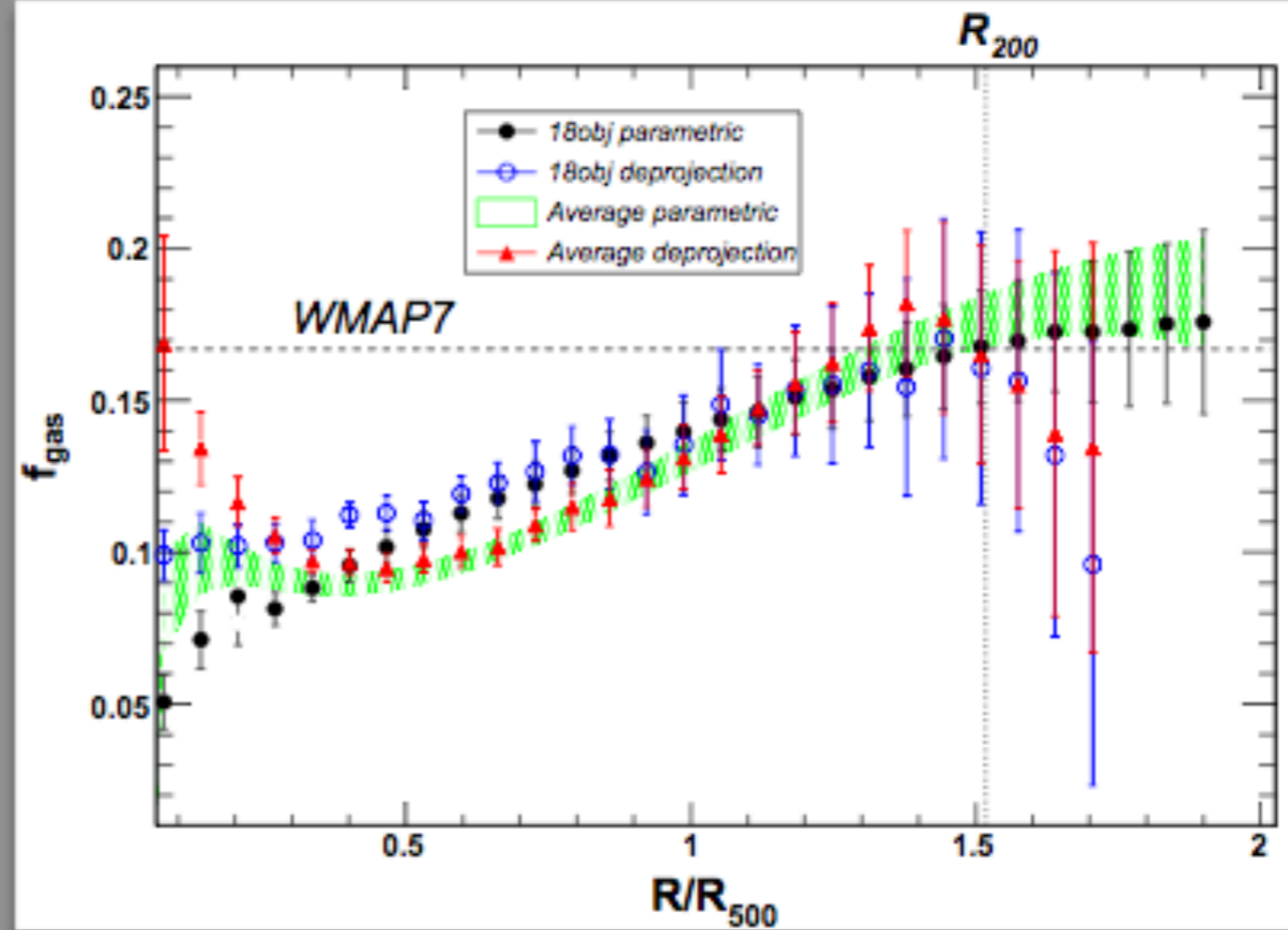
Typical result:

clusters have progressively more gas than stars at higher masses

Rasheed (2010)



Typical result:
the baryon fraction increases with radius

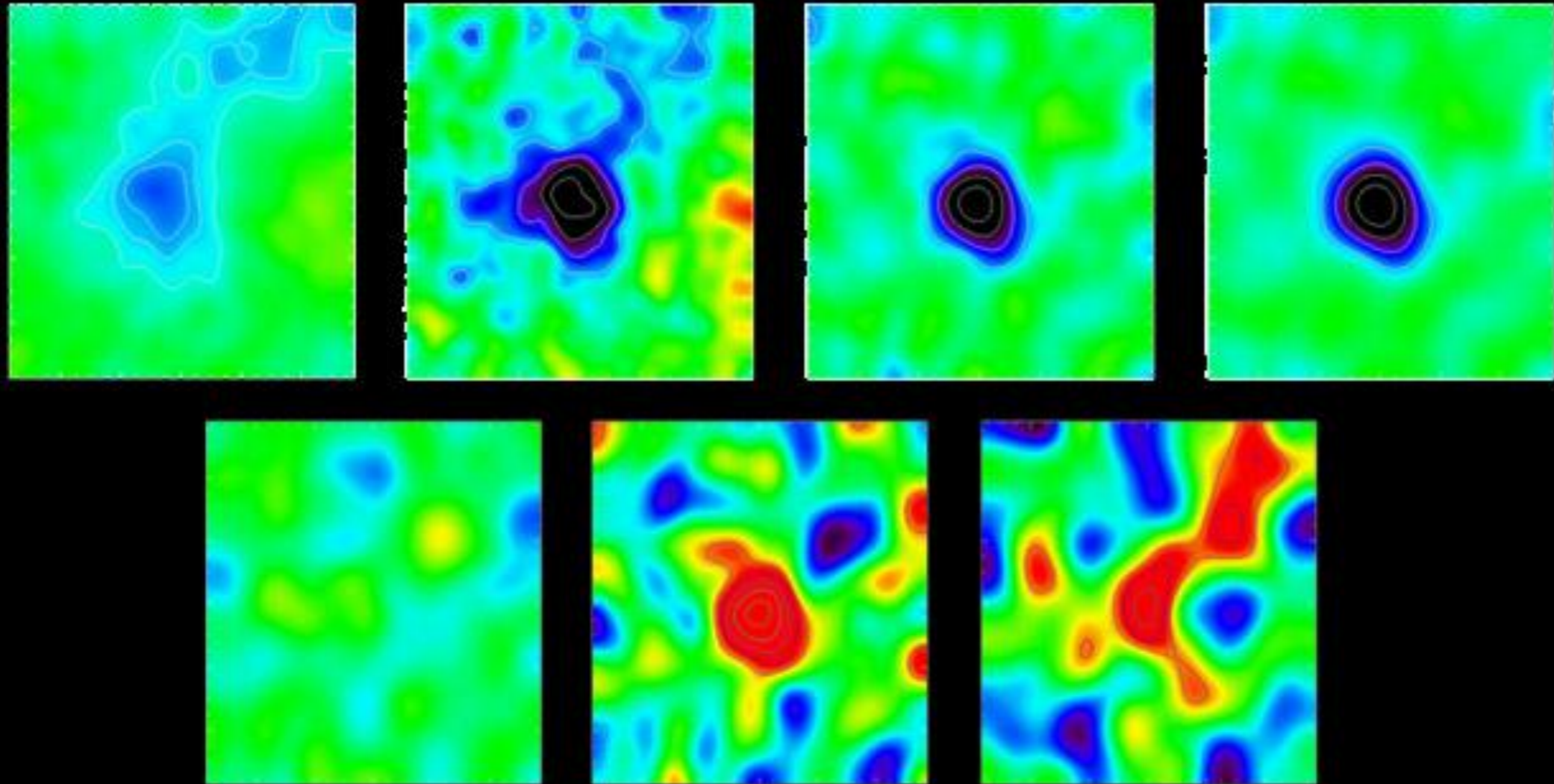


Typical result:

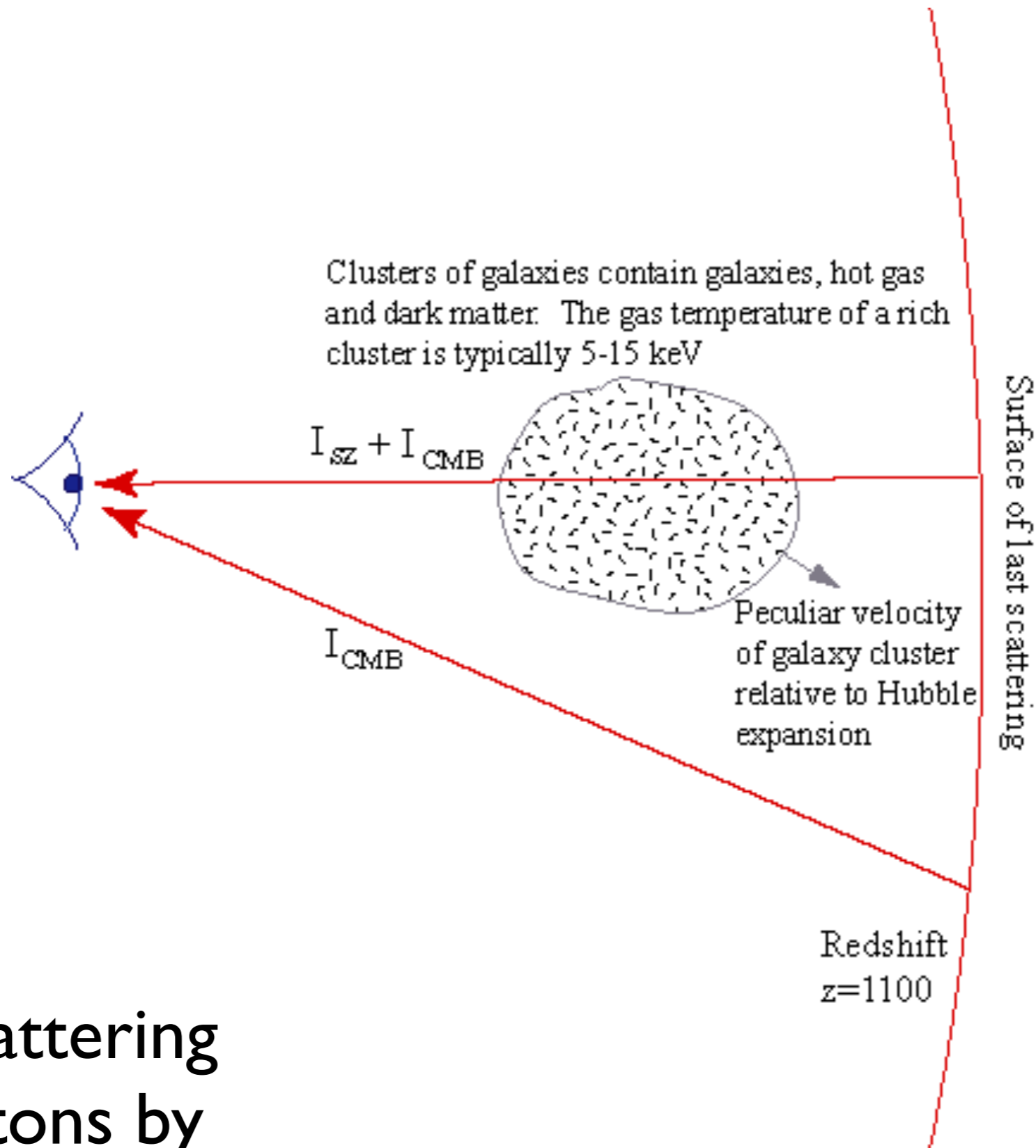
ICM gas outweighs the stars by factor of ~ 6 ;
 outweighed by dark matter by the same factor

There seems to be a missing baryon problem towards the centers of clusters

SUNYAEV-ZEL'DOVICH EFFECT



SUNYAEV-ZEL'DOVICH EFFECT



Compton scattering
of CMB photons by
hot ICM plasma

frequency dependent change in intensity

$$\frac{\delta I_{nu}}{I_\nu} = -y \frac{x e^x}{e^x - 1} \left[4 - x \coth \left(\frac{x}{2} \right) \right]$$

where $x = \frac{h\nu}{kT_{rad}}$ and $y = \int \sigma_T n_e \frac{kT_g}{m_e c^2} d\ell$

\uparrow
CMB

\uparrow
electron density

\uparrow
Thomson scattering cross-section

y is the Compton y -parameter which quantifies how much effect the plasma has

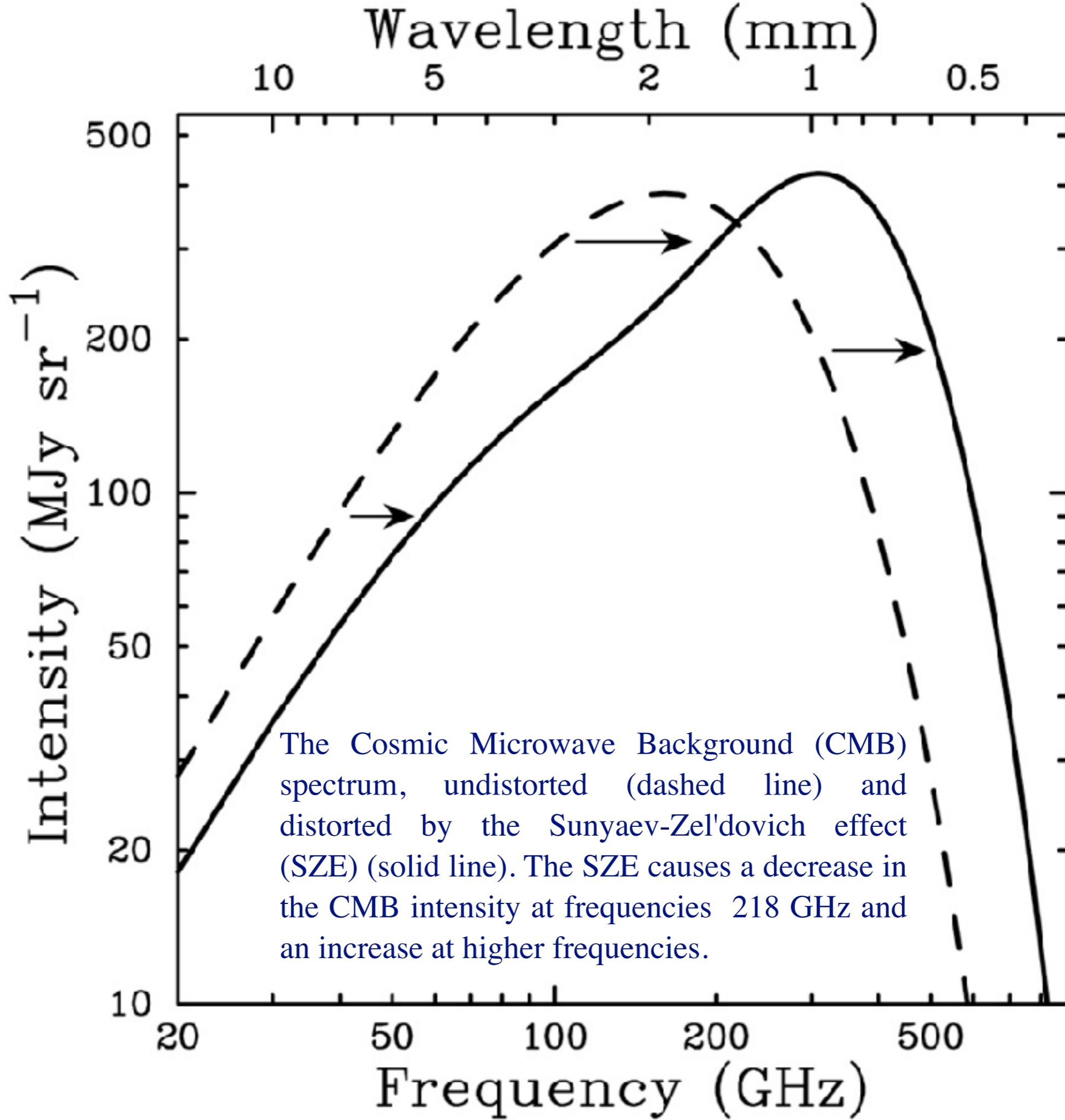
frequency dependent change in intensity

$$\frac{\delta I_{nu}}{I_\nu} = -y \frac{x e^x}{e^x - 1} \left[4 - x \coth \left(\frac{x}{2} \right) \right]$$

where $x = \frac{h\nu}{kT_{rad}}$ and $y = \int \sigma_T n_e \frac{kT_g}{m_e c^2} d\ell$

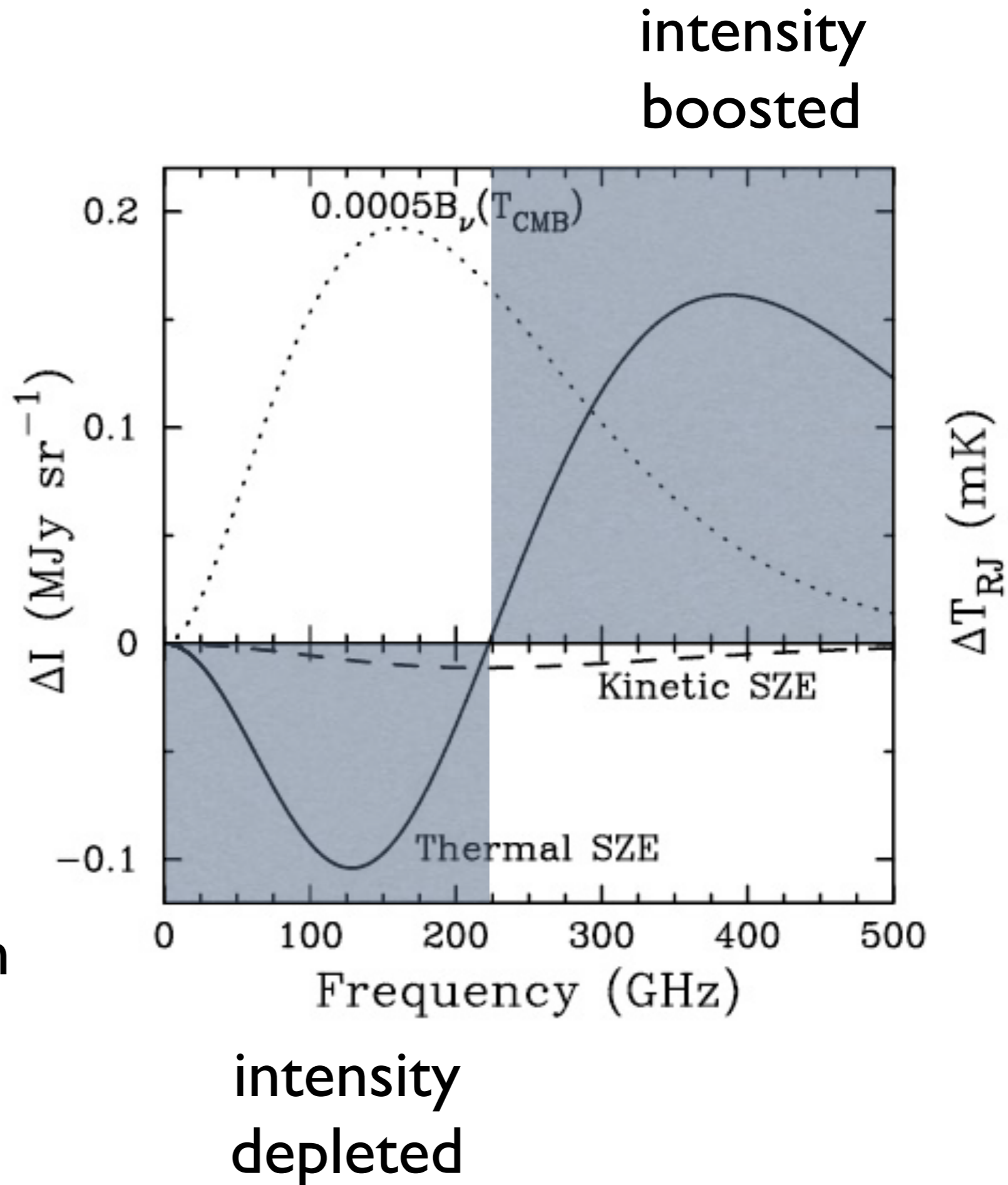
at low frequency in the Rayleigh-Jeans tail,

$$\frac{\delta I}{I} = \frac{\delta T}{T} = -2y$$



Thermal SZ effect from Compton scattering of CMB photons by cluster plasma

Kinematic SZ effect from peculiar velocity of cluster wrt CMB frame



SUNYAEV-ZEL'DOVICH EFFECT

detected by Planck

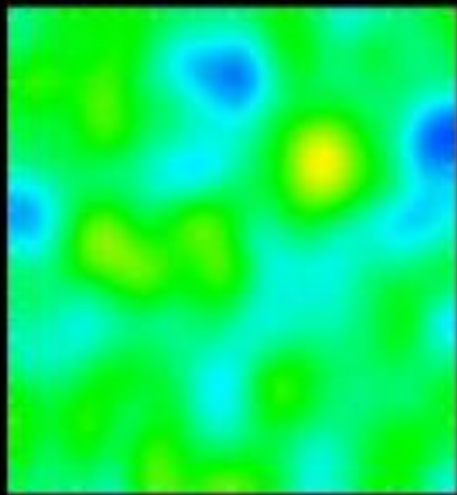
44 GHz

70 GHz

100 GHz

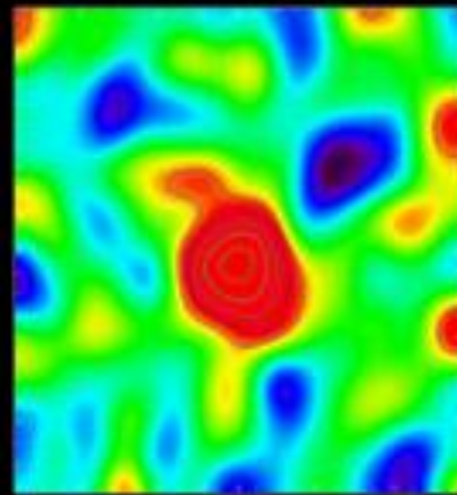
143 GHz

low
frequency
deficit

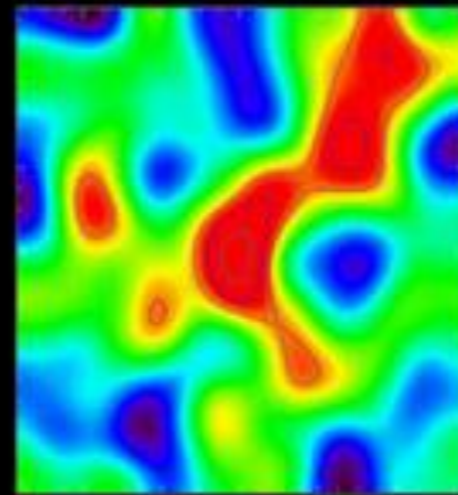


217 GHz

cross-over
frequency



353 GHz



545 GHz

high
frequency
excess

Wavelength (mm)

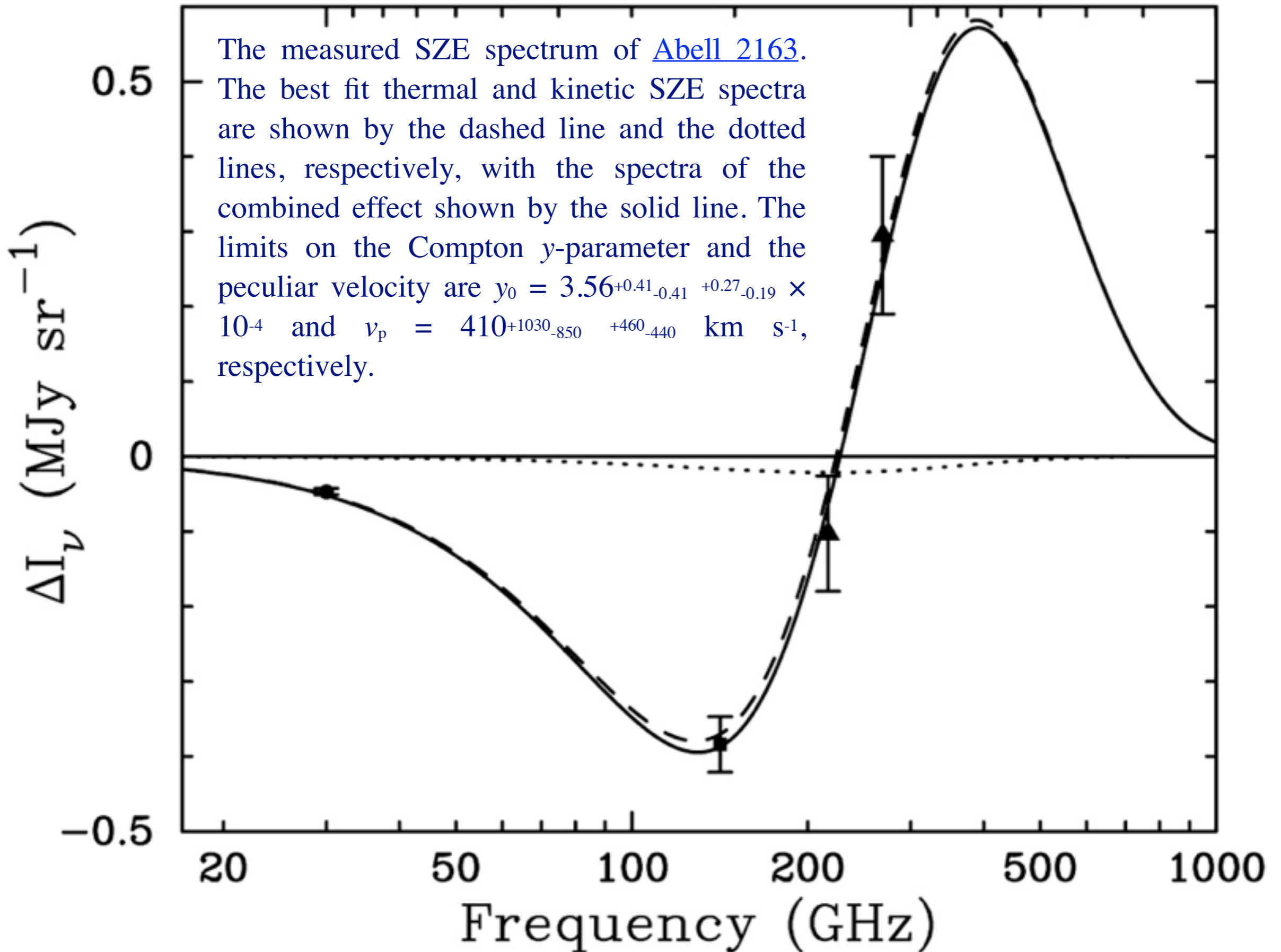
10

5

2

1

0.5



integrated change in CMB temperature

$$\int \Delta T d\Omega \propto \frac{N_e \langle T_e \rangle}{D_A^2} \propto \frac{M \langle T_e \rangle}{D_A^2}$$

depends on the total number of electrons, their temperature, and the area they subtend on the sky. In effect measures Pressure, or mass if T known.

D_A is the angular diameter distance.

At high z , it varies slowly, while the density increases as $(1+z)^3$

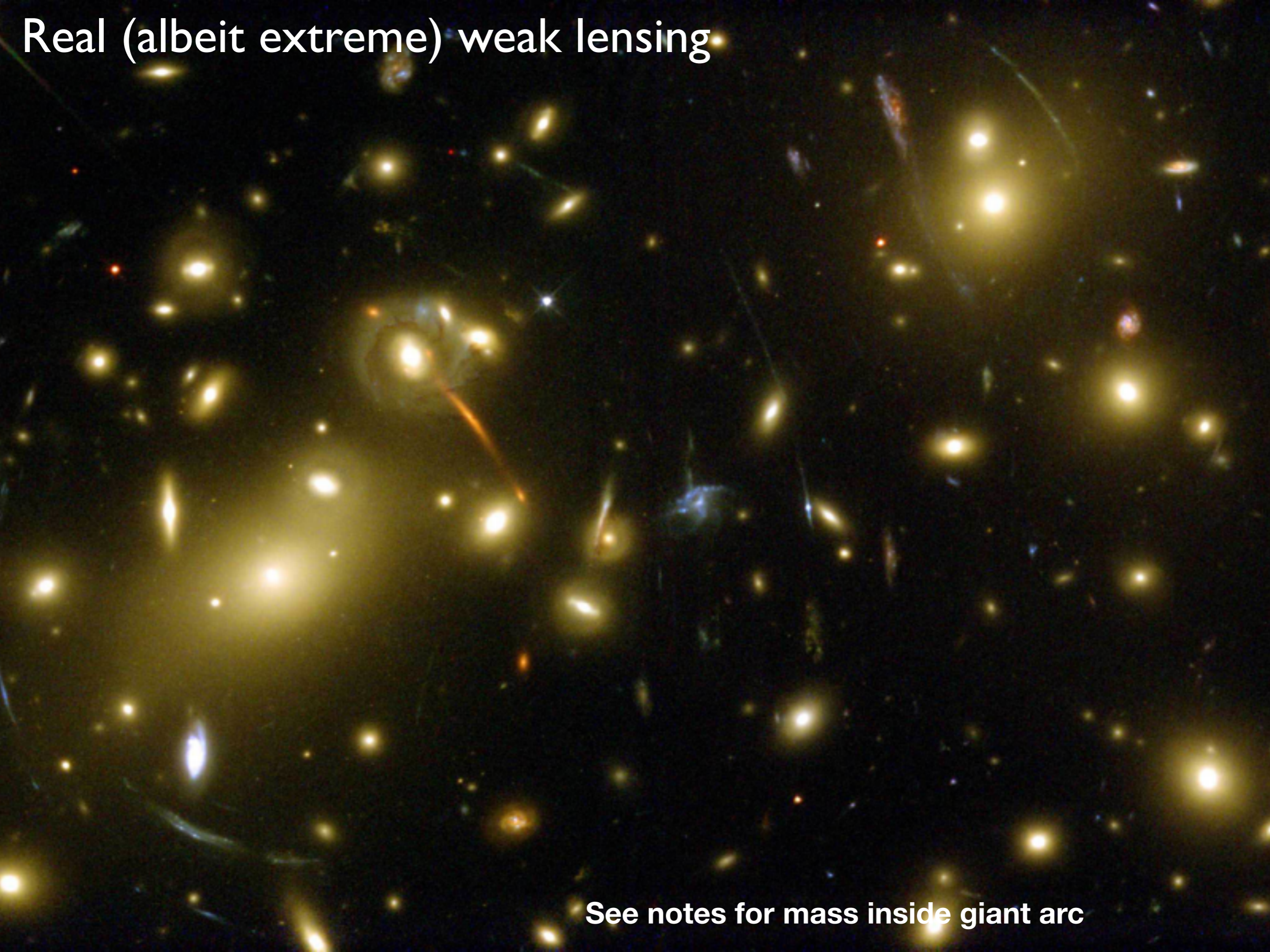
... SZ effect weak, but nearly independent of redshift!

Fake illustration of weak lensing



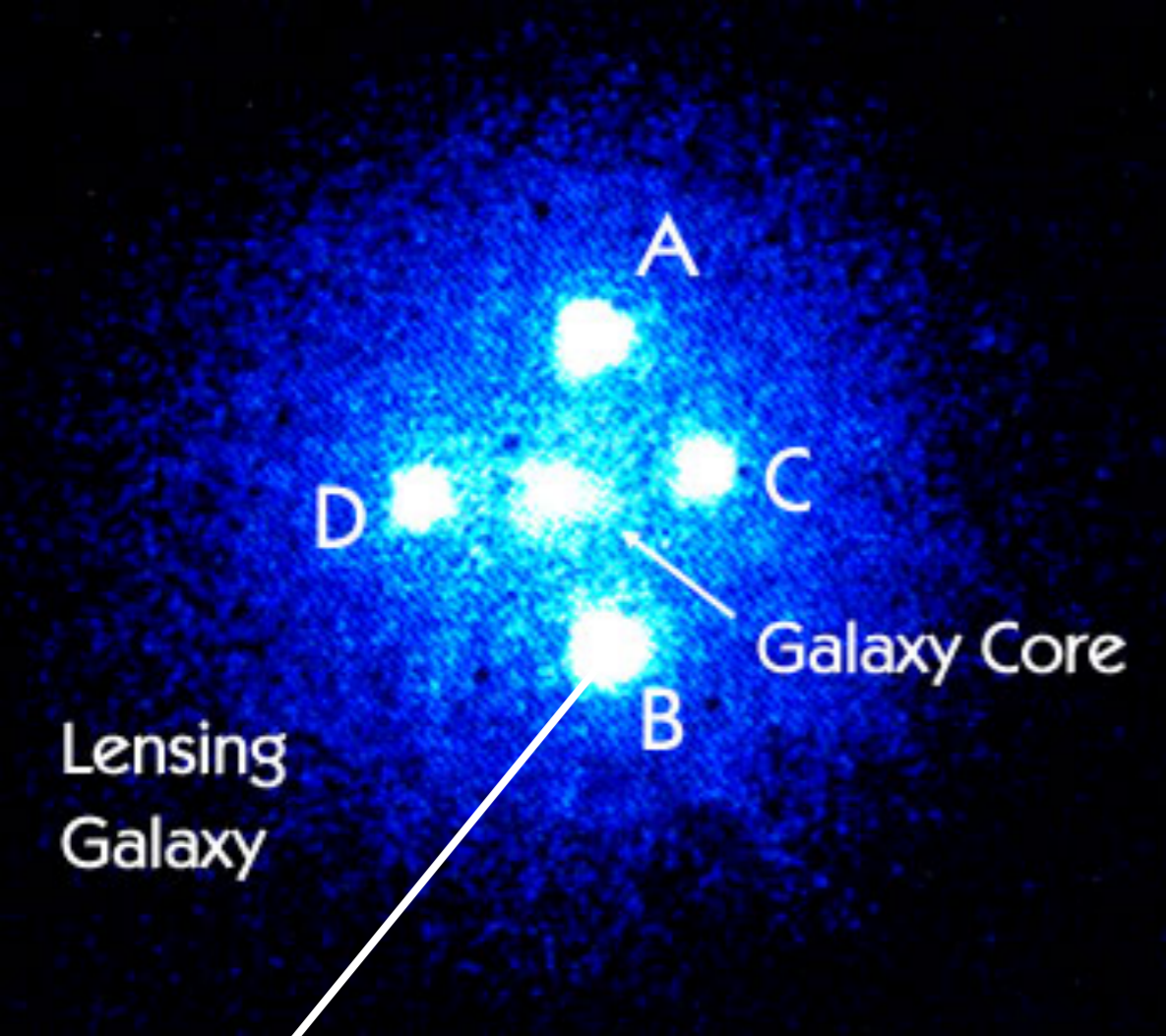
See notes for mass inside giant arc

Real (albeit extreme) weak lensing

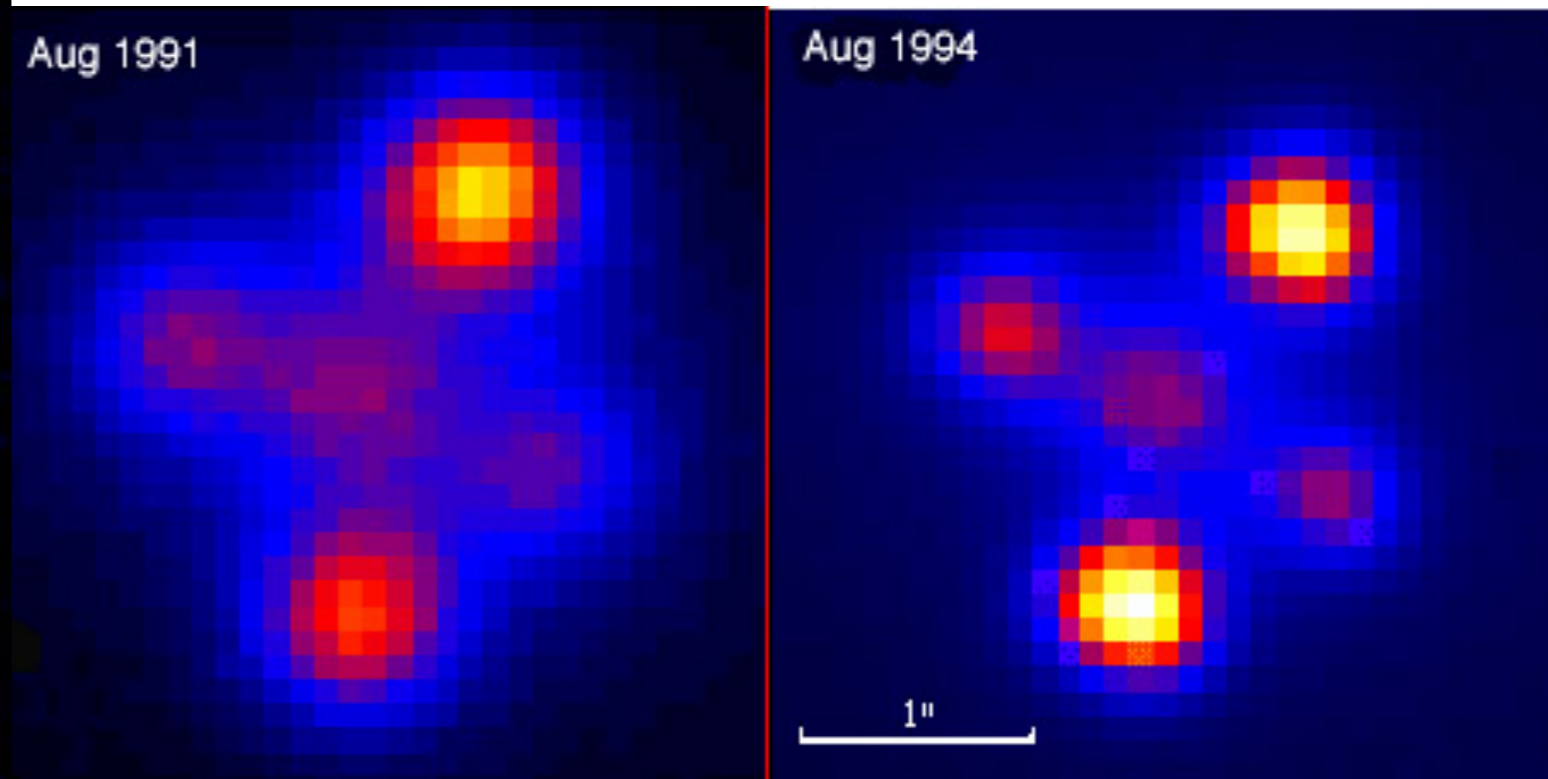


See notes for mass inside giant arc

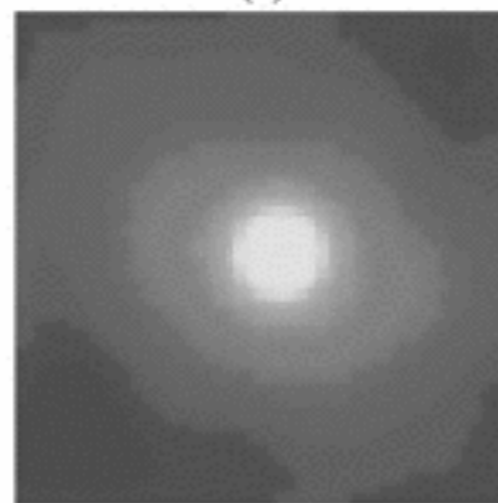
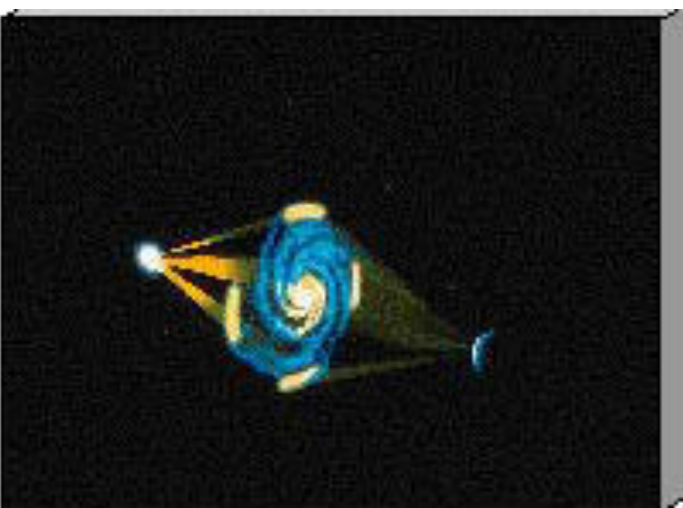
Strong lensing: Einstein Cross



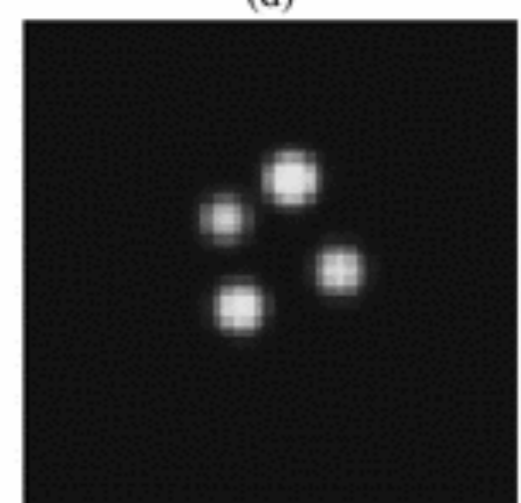
ABCD: same QSO seen 4 times



time variable multiple QSO image

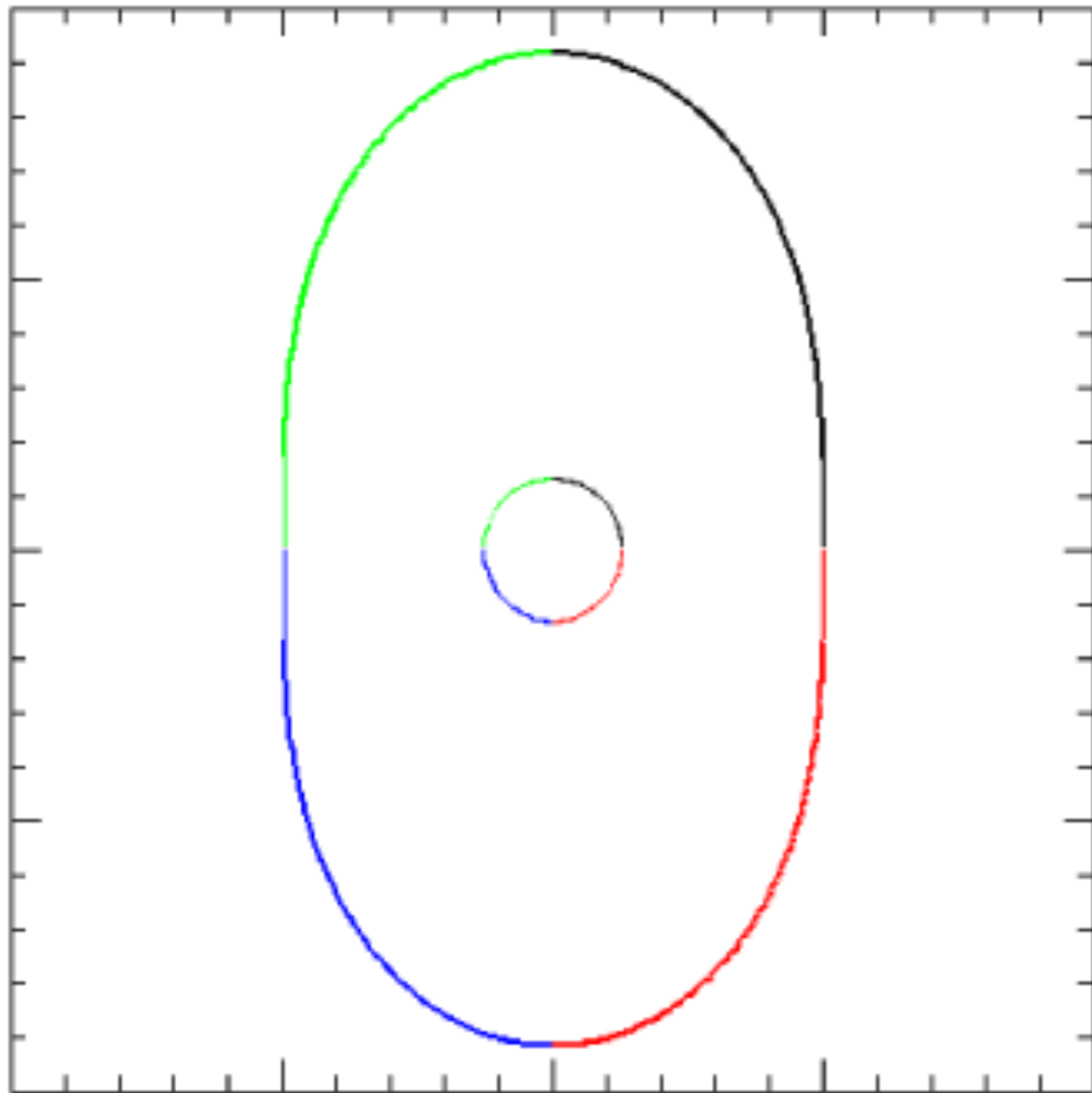


lensing galaxy



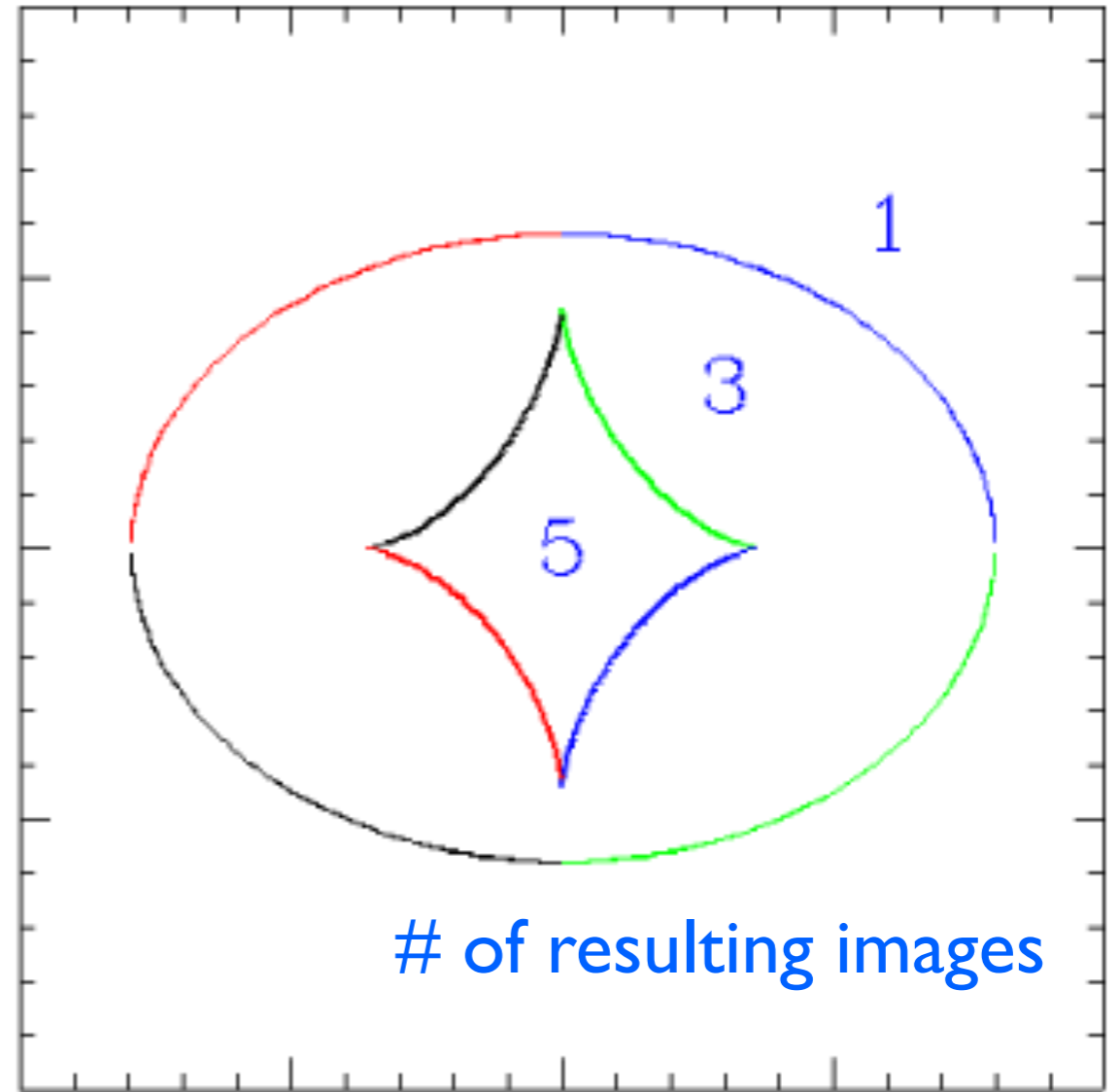
lensed QSO

Lens plane



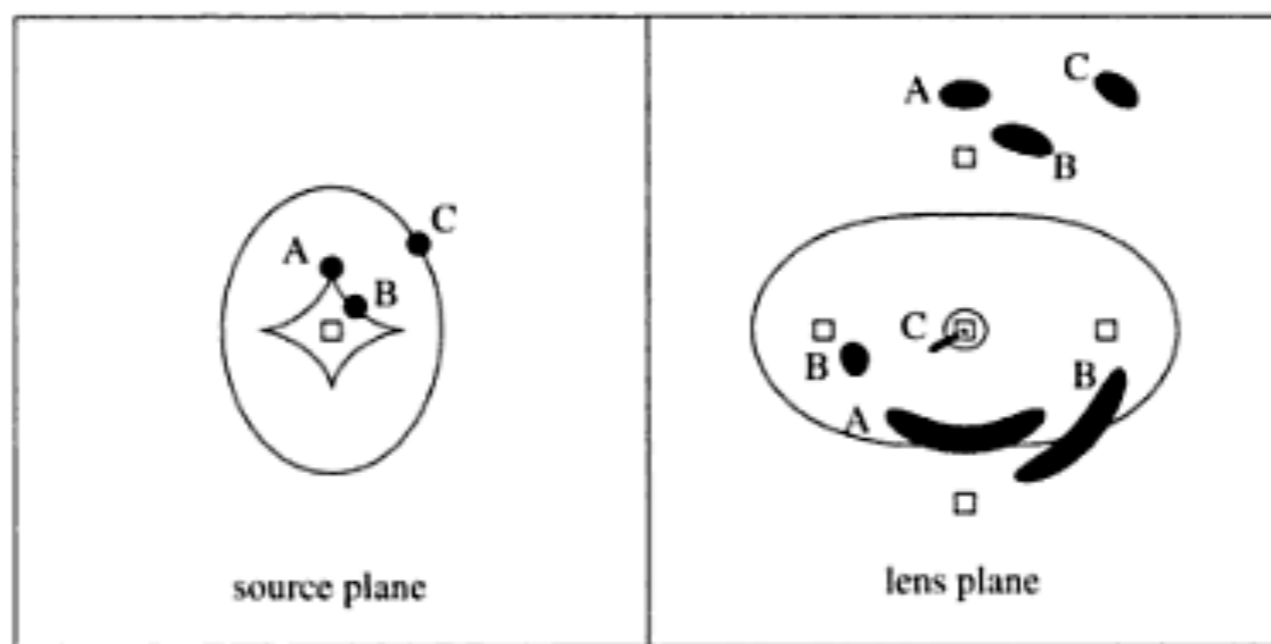
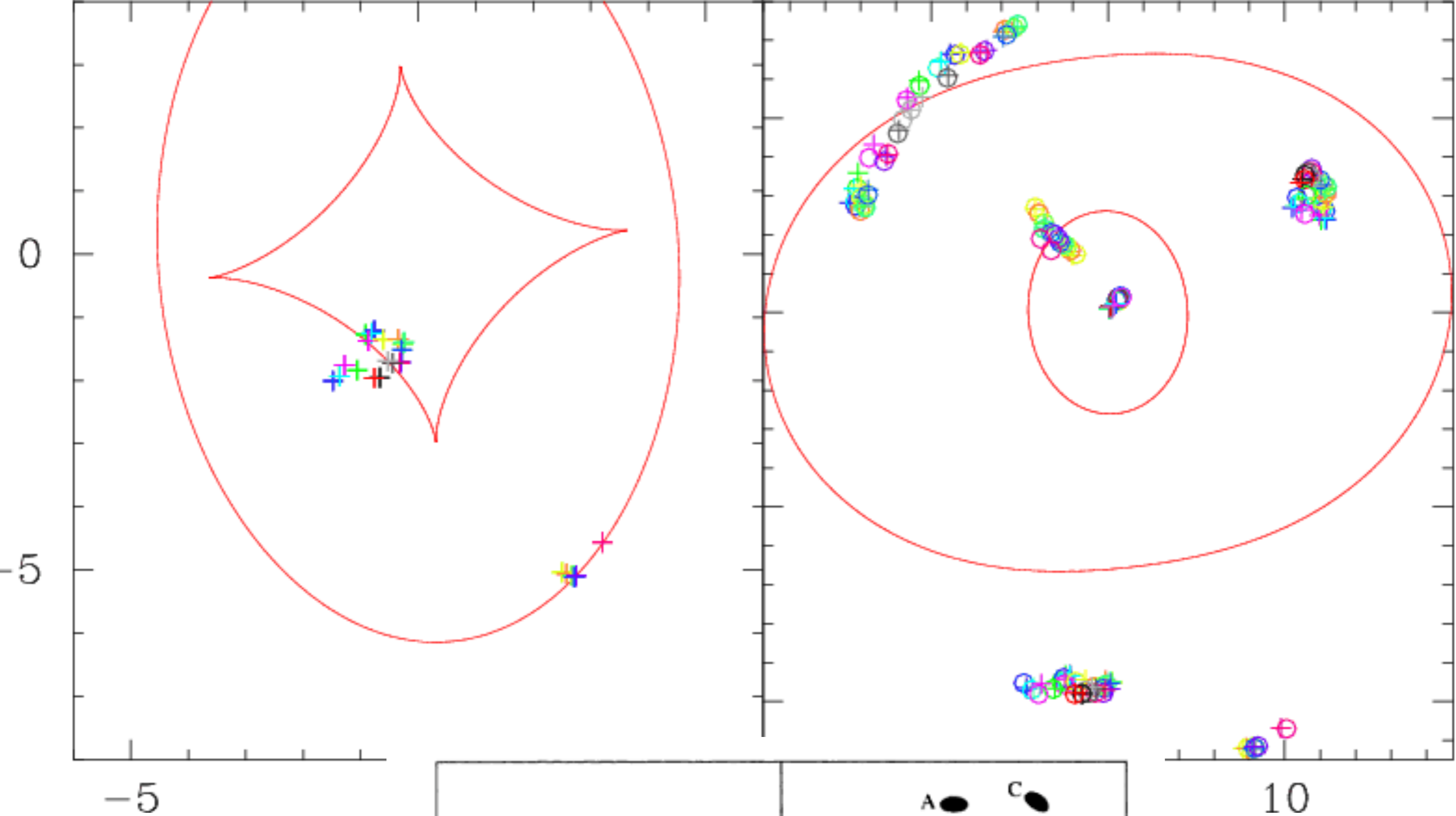
critical curves

Source plane

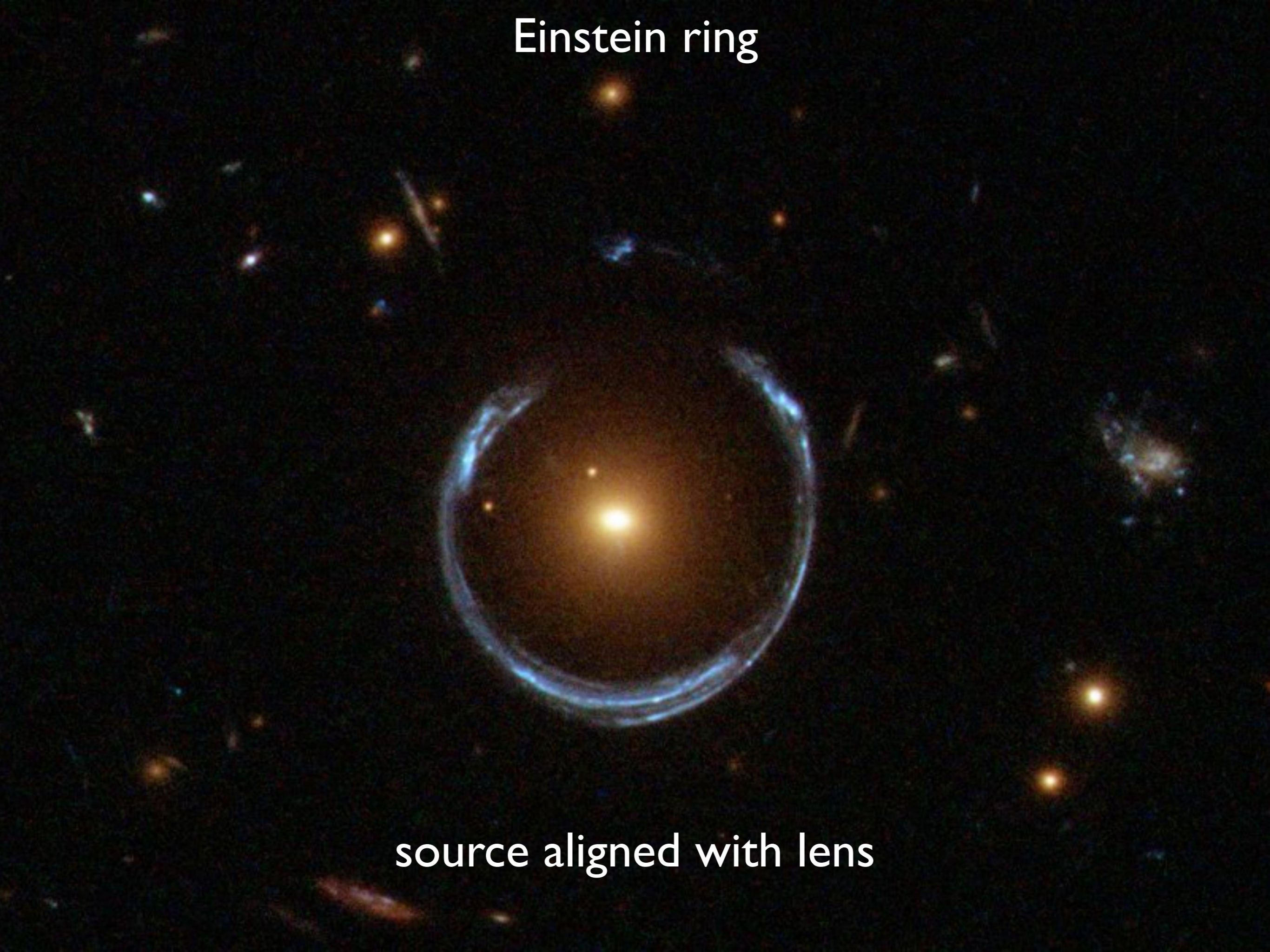


of resulting images

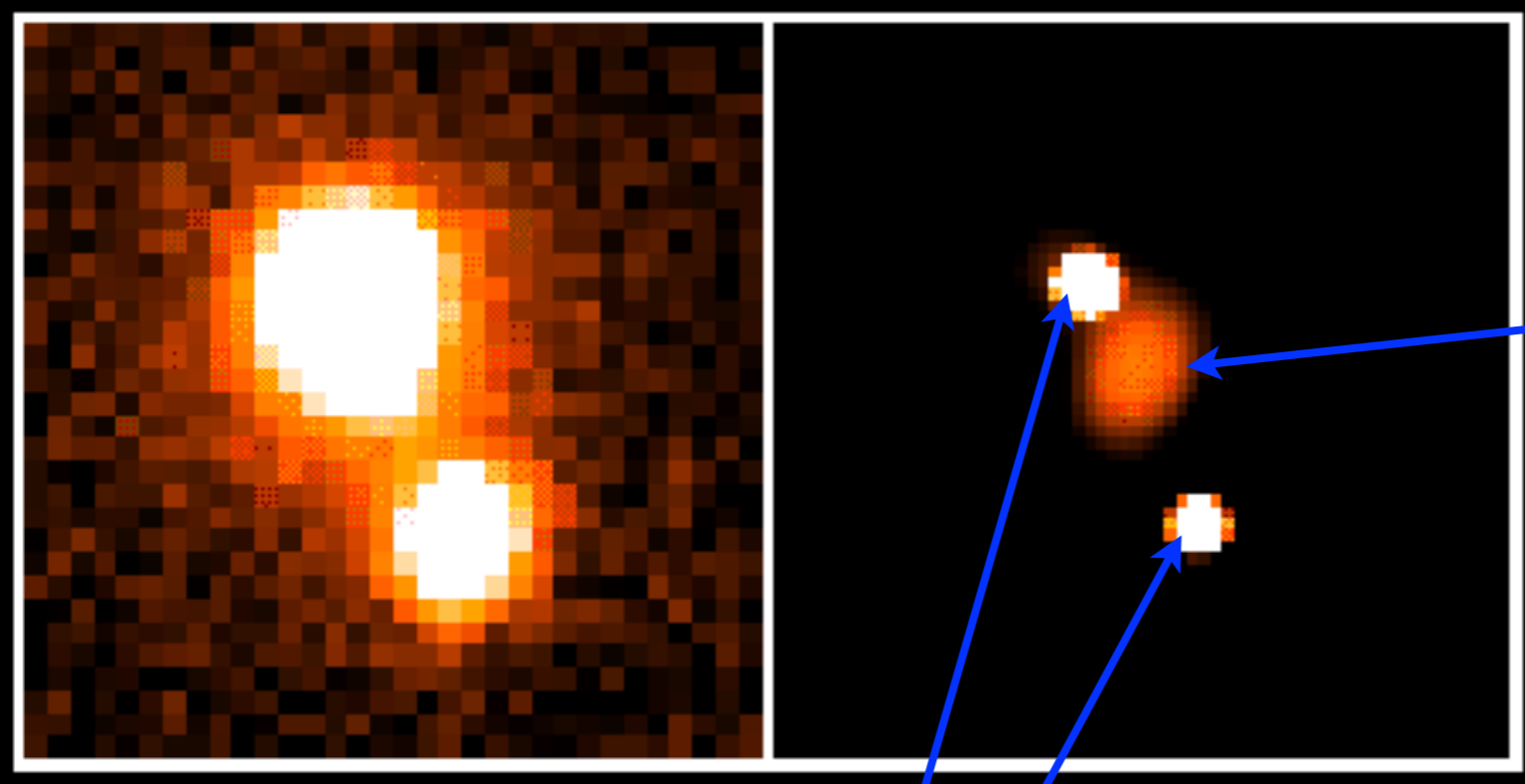
caustics



Einstein ring

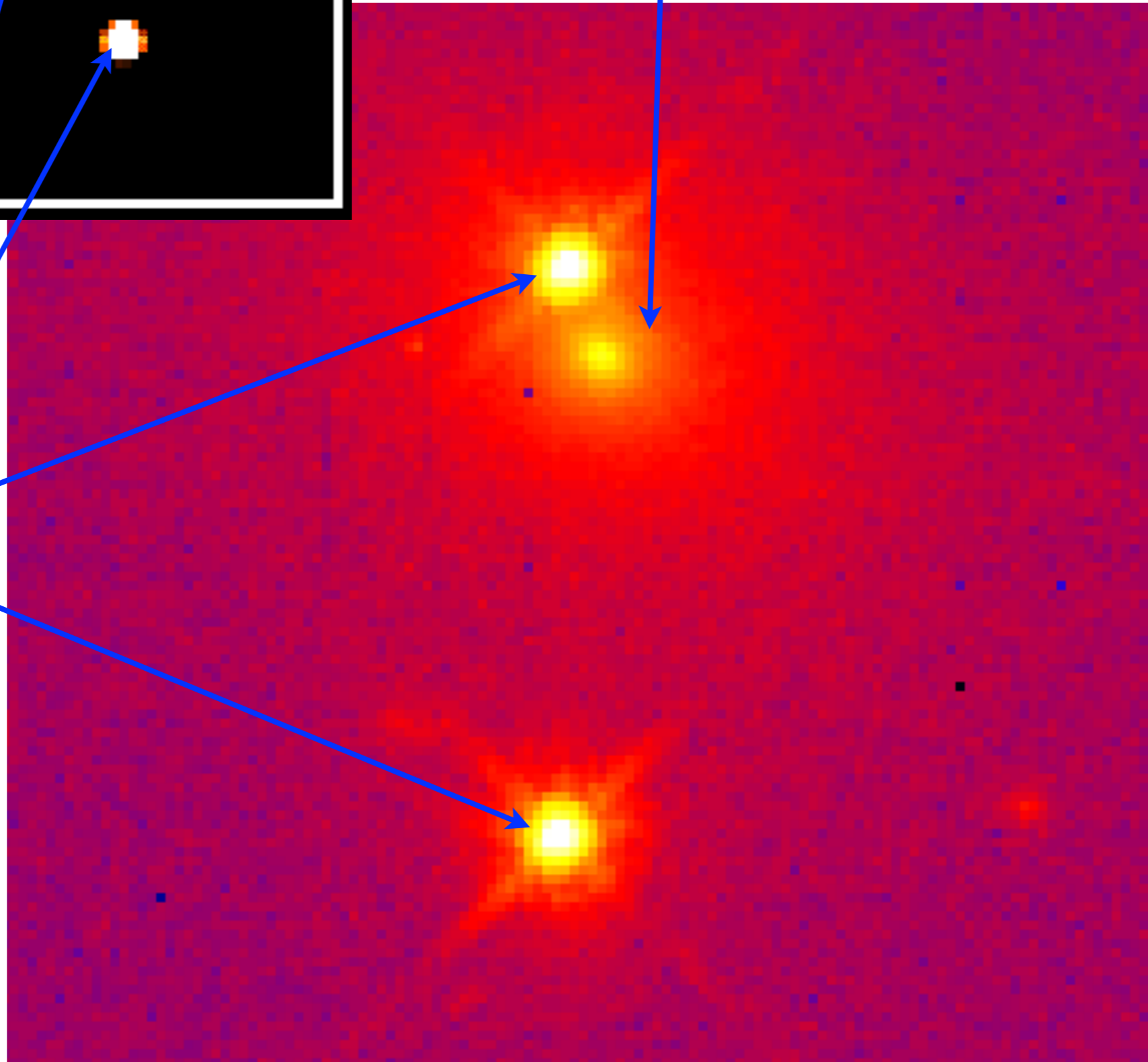


source aligned with lens



Lensing galaxy

Lensed images

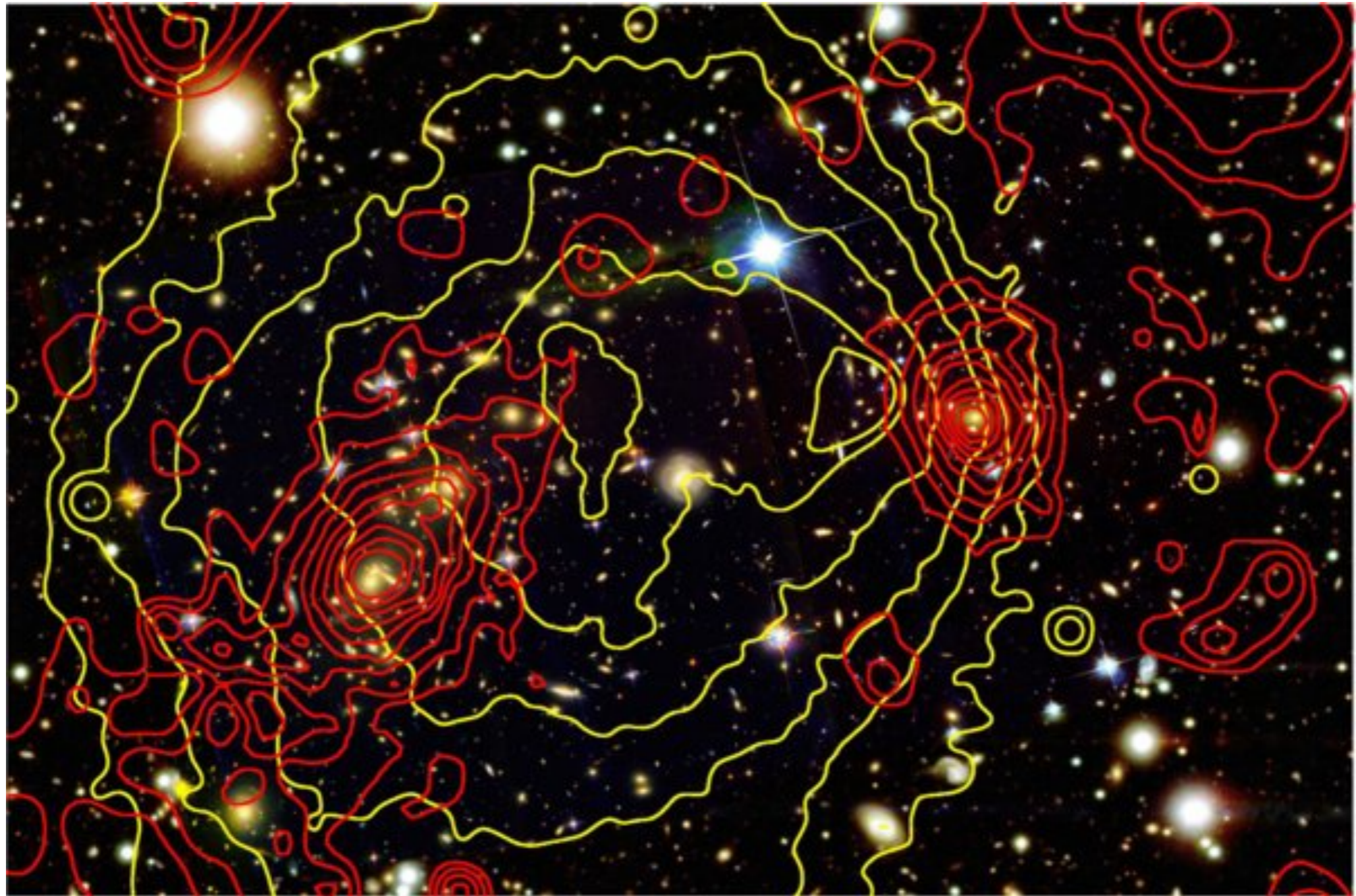


Bullet cluster (press release version)



Bullet cluster (Bradac et al. 2009)

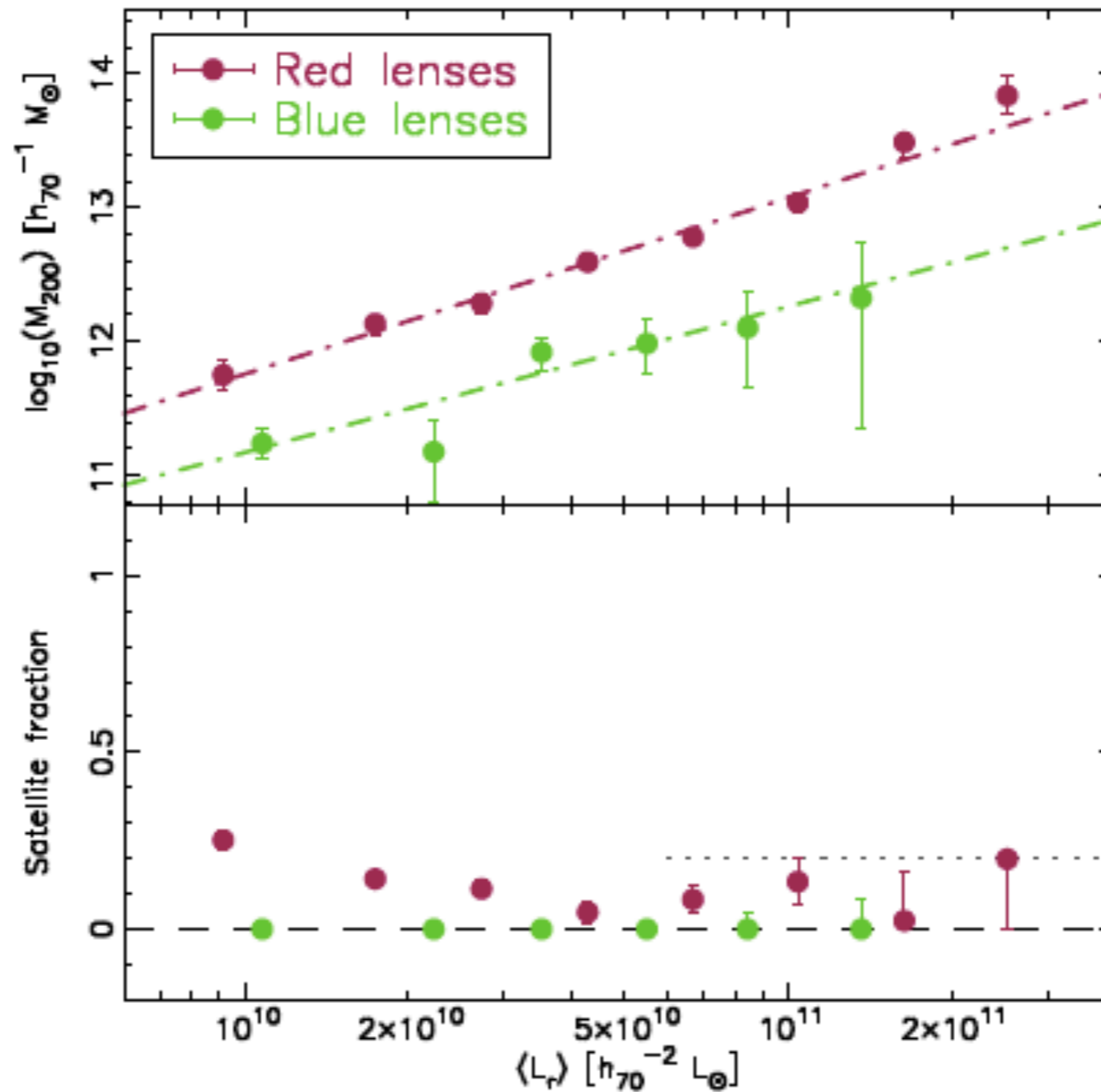
X-ray: yellow contours



gravitational (strong+weak) lensing: red contours

Velander et al (2013) weak gravitational lensing

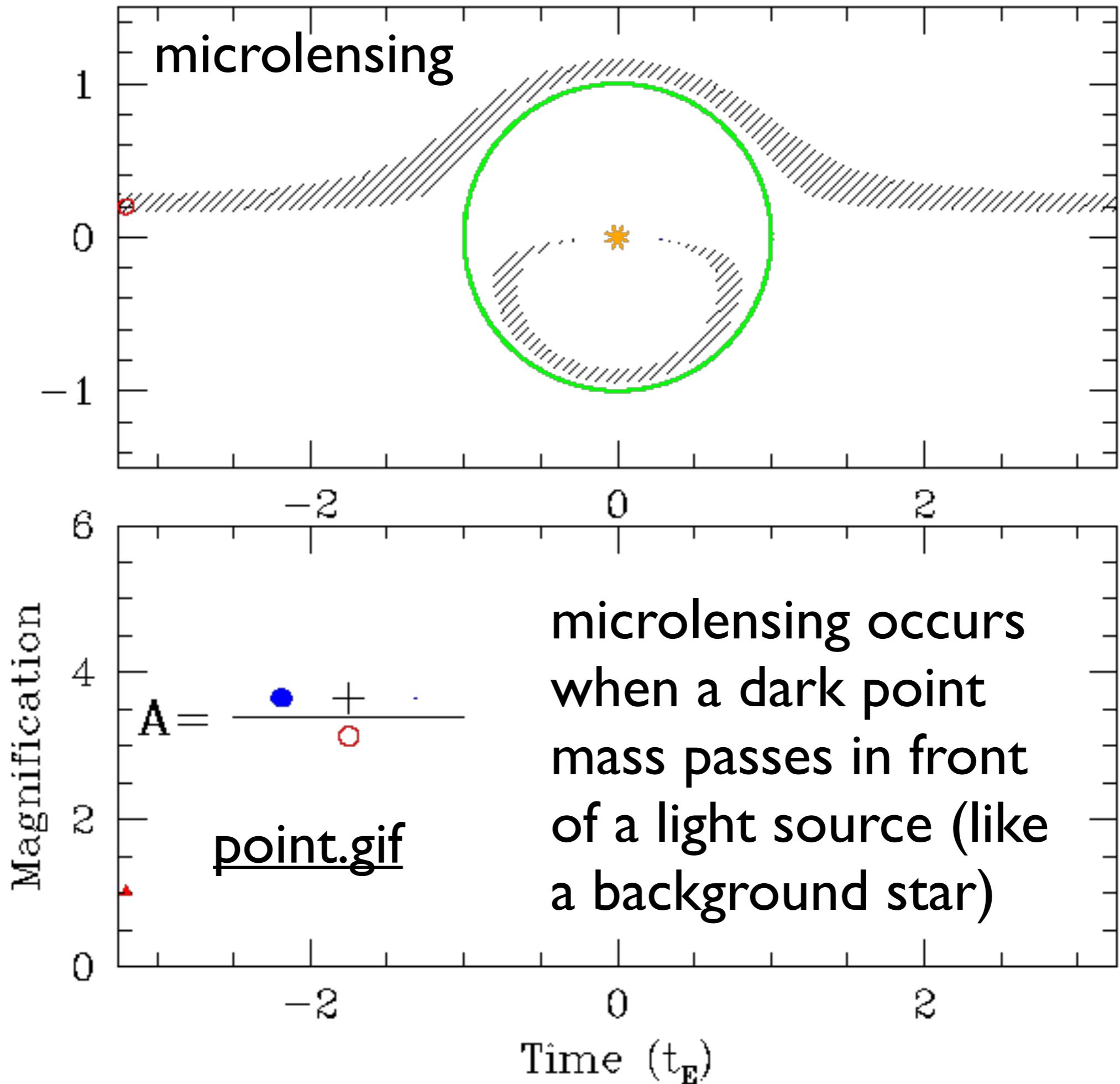
BIG SCALES



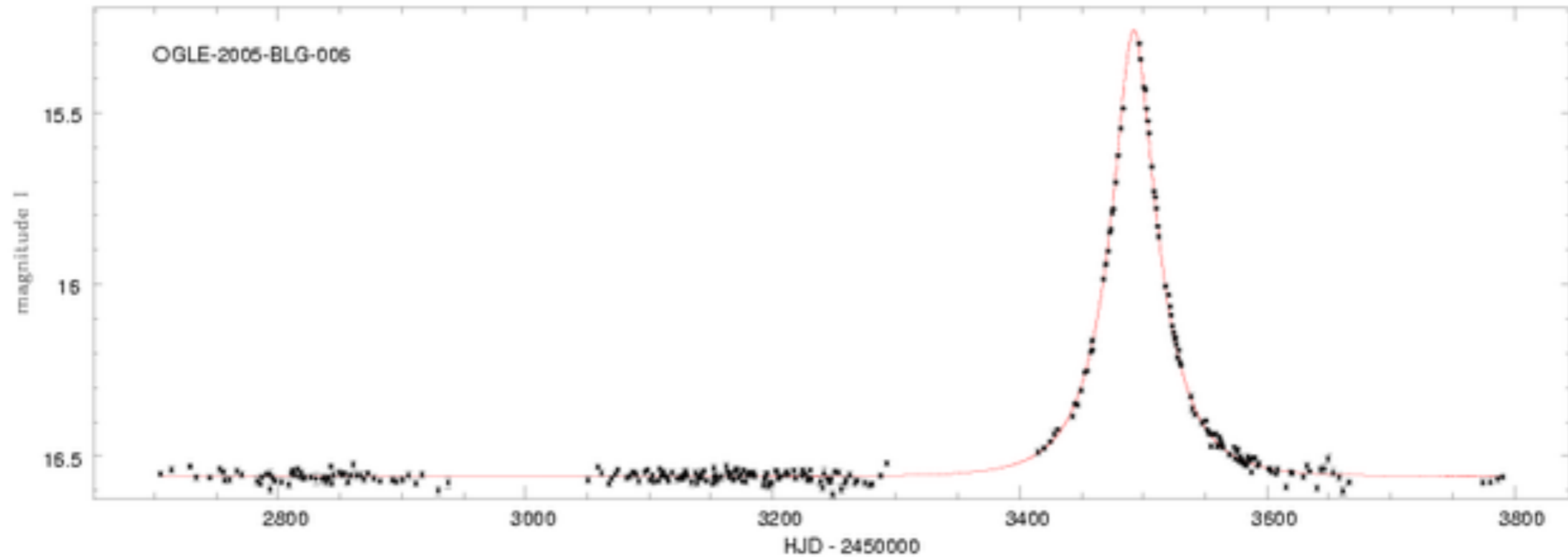
**Weak lensing
provides a statistical
constraint on the
total halo mass**

$$M_{200} = 119 L_r^{1.32} \quad \text{for red galaxies}$$

SMALL SCALES

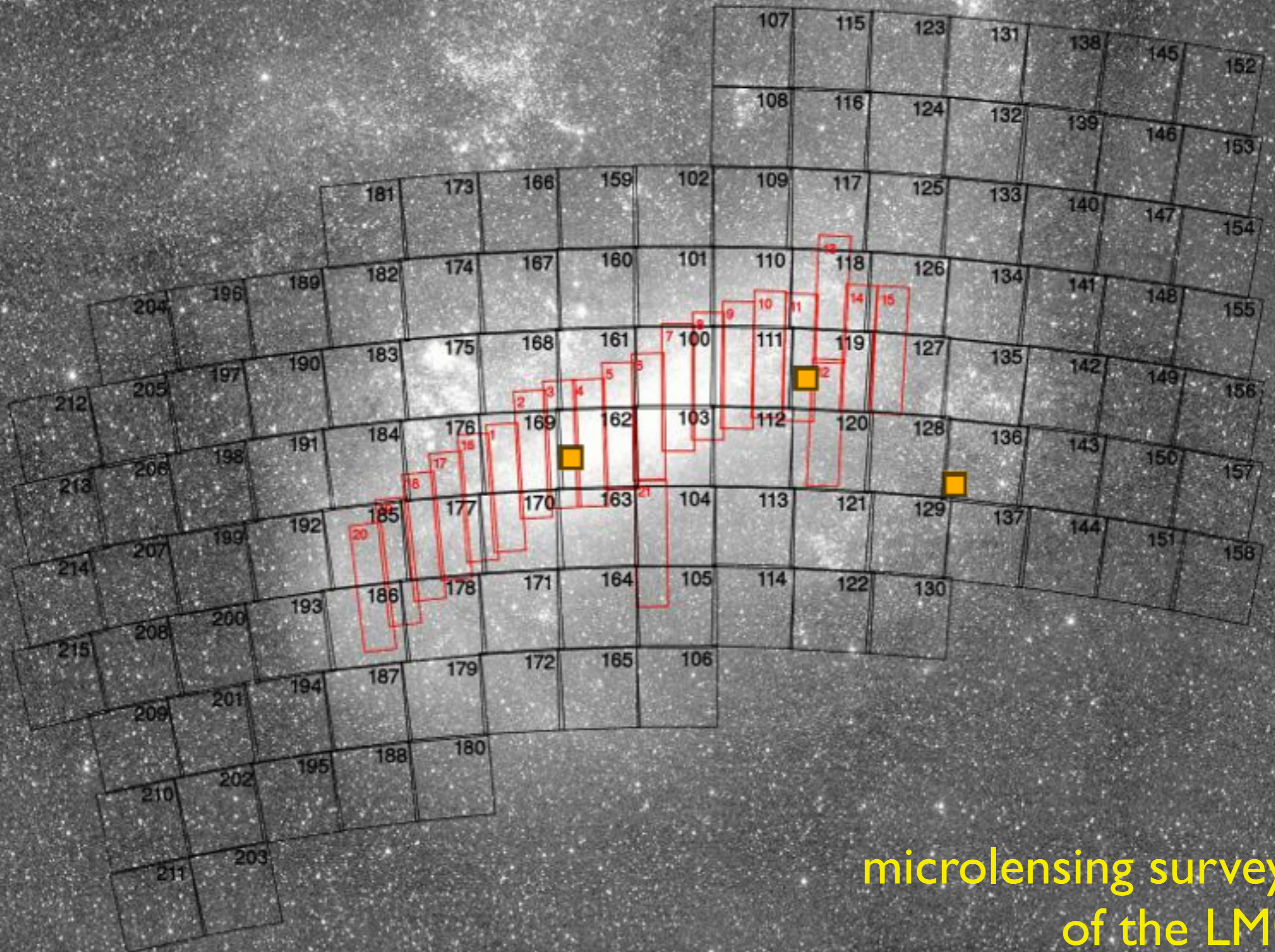


microlensing even observed by OGLE



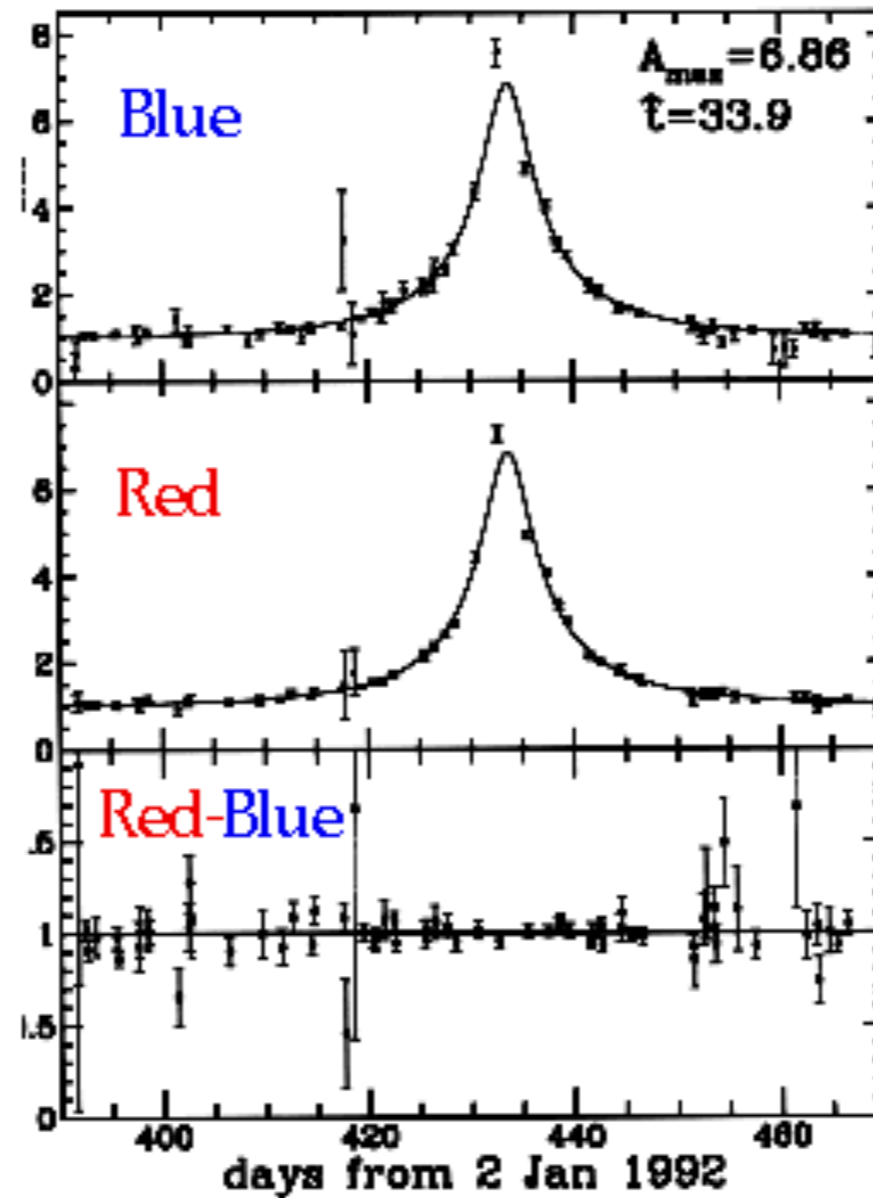
Microlensing surveys:
MACHO
EROS
OGLE

stare at LMC/SMC to look for microlensing events due to intervening dark matter. Sensitive to brown dwarfs.



microlensing surveys
of the LMC

microlensing events achromatic



should also be symmetric in time
(unless there is a companion planet)

Planet detections by microlensing

